Catalytic Conversion of Glucose to 5-Hydroxymethylfurfural using Zirconium-Containing Metal-Organic Frameworks

by

©Jue Gong

A dissertation submitted to the School of Graduate Studies in partial fulfillment of the requirements for the degree of

M.Sc.

Department of Chemistry

Memorial University of Newfoundland

July 2018

St. John's Newfoundland

Abstract

5-hydroxymethylfurfural (5-HMF) can be obtained by the catalytic dehydration of glucose or fructose using different homogeneous or heterogeneous catalysts. In my research project, four closely related zirconium-containing Metal-Organic Frameworks (MOFs) were chosen as catalysts for the conversion of glucose to 5-HMF due to their chemical and thermal stability as well as the Lewis acidity of zirconium. The initial research focused on the use of UiO-66-X (X= H, NH_2 and SO_3H), optimization of reaction conditions and investigation of the relationship between their catalytic activity and properties. The highest yield of 5-HMF (28%) was obtained using UiO-66 under the optimal reaction conditions. In catalyst recycling experiments, UiO-66 could be re-used after five runs with a small reduction in the yield of-5-HMF. We assumed that this is due to the formation of humin after reaction. Thus, used UiO-66 catalyst, named UiO-66-humin, was characterized by several techniques such as PXRD, FT-IR, ^{13}C Solid State NMR spectroscopy, and N_2 adsorption measurements. MOF 808 was another potential candidate for the conversion of glucose since it possesses lower connectivity (6-connected) with larger surface area compared with UiO-66. MOF 808 was synthesized via a solvothermal method and characterized by PXRD and N_2 adsorption measurements. Notably, MOF 808 afforded higher yields of 5-HMF when compared with UiO-66-X.

Acknowledgements

I would like to thank Dr. Francesca Kerton for trusting me, accepting me, providing the graduate position for me and for training me in the laboratory. From this, I can skillfully do my research and freely 'play' with several instruments. Fran is an easygoing and kind person so I never feel nervous or stressed when I talk with her. What's more, she was patient and gave me lots of useful and valuable suggestions during my Masters career. Under her supervision, what I have learned from Fran in the past two years is not only chemistry knowledge but also the philosophy of being a chemist. It has been a pleasure to work with her over last two years.

I would also like to thank Dr. Michael Katz for guiding me when I started my Masters at Memorial University of Newfoundland. Mike is my co-supervisor and he helped me a lot with regards to metal-organic frameworks (MOFs) synthesis and their crystal structure analysis. Without his help, I could not succeed in my research project. Moreover, I want to say thanks to my lovely Green Chemistry and Catalysis group members. I enjoyed time in the lab or office with my colleagues in the past two years. In particular, I would like to thank my two senior group members, Yi Liu and George Margoutidis, for helping me in the field of GC-MS and 5-HMF synthesis since their research projects were closely related to mine more or less. Overall, I am so happy that I was a member of Fran's group.

I would further like to thank Dr. Christopher Kozak and Dr. Christina Bottaro.

From their class, I learned a lot of useful knowledge of catalysis and analytical techniques. I appreciate Nicholas Ryan for FT-IR training, Wanda Aylward for PXRD data collection, Mason Lawrence for N_2 adsorption tests and Celine Schneider for NMR 300 and 500 instrument training as well as acquiring Solid-State NMR spectra.

I would like to thank the Department of Chemistry at Memorial University of Newfoundland for providing me with a perfect study and working environment over the past two years. Every person was pretty accommodating and it was easy to talk and ask questions in the department. I would like to acknowledge the Natural Sciences and Engineering Research Council of Canada (NSERC), Canada Foundation for Innovation (CFI) and Memorial University of Newfoundland for funding.

Last but not least, this is my fifth year in Canada and I would like to thank my parents and friends for their support and encouragement over the past five years.

Table of Contents

Abstract **ii**

Acknowledgments **iii**

List of Tables **vii**

List of Figures **x**

List of Abbreviations and Symbols **xi**

1 Introduction **1**

1.1 Biomass Feedstocks 1

1.2 5-Hydroxymethylfurfural (5-HMF) and Its Applications 6

1.3 Metal-Organic Frameworks (MOFs) Introduction 17

1.4 Catalytic Conversion of Carbohydrates to 5-HMF using MOFs 27

1.5 Summary 30

References 31

Co-authorship Statement **49**

2 Materials and Methods **50**

2.1 Materials, Reagents and Instrumentation 50

2.2 Synthesis of MOFs 51
2.3 Catalytic Conversion of Glucose to 5-HMF 52
2.4 Recycling Experiment and Characterization of Humin 53
References 53

3 Results and Discussion **55**
3.1 Dehydration of Glucose to 5-HMF using UiO-66 and its analogues . . 55
3.2 Optimization of Reaction Conditions 61
3.3 Recycling Test 66
3.4 Characterization of Humin on MOF Surface 68
3.5 Dehydration of Glucose to 5-HMF using MOF 808 74
References 79

4 Conclusions **86**

List of Tables

1.1 Conversion of carbohydrates to 5-HMF using homogeneous catalysts . 10

1.2 Conversion of carbohydrates to 5-HMF using heterogeneous catalysts 13

3.1 Yields for glucose conversion to 5-HMF. 59

3.2 Optimization of reaction time, catalyst loading and temperature of UiO-66 for the conversion of glucose to 5-HMF[a,b] 61

3.3 Comparison of glucose conversion to 5-HMF using UiO-66 and literature reports using three different MOFs 67

List of Figures

1.1 Single repeating unit of cellulose. 2

1.2 Structure of hemicellulose. 3

1.3 Structures of three lignin precursors: (a) *p*-coumaryl alcohol; (b) coniferyl alcohol; (c) sinapyl alcohol. 4

1.4 The schematic illustration of categories of biomass. 5

1.5 Applications of 5-HMF as a building block. 8

1.6 Three products from oxidation of 5-HMF. 15

1.7 Two products of reduction of the formyl group of 5-HMF. 16

1.8 Molecular structure of 2,5-dimethylfuran. 16

1.9 Schematic illustration of metal-organic frameworks (MOFs). 18

1.10 Graphical illustration of different approaches to MOF synthesis . . . 19

1.11 Two-step modification process for producing Au(III)-MOF. Zn, green; O, red; C, light blue; N, deep blue; Au, yellow; Cl, white. H atoms are omitted for clarity. Reprinted from [99], Copyright (2009), with permission from Elsevier. 22

1.12 Schematic illustration of (a) a "Classic" MOF with only coordinative groups (L) and (b) a MOF having both coordinative (L_1) and reactive (L_2) groups. Reprinted with permission from [95]. Copyright (2010) American Chemical Society. 23

1.13 Equation for preparation of the POST-1 homochiral MOF (CO_2R = organic carboxylate anions). 24
1.14 Schematic illustration of the Knoevenagel condensation reaction. . . . 24
1.15 The structure of 4-btapa. 26
1.16 Illustration of Knoevenagel condensation reaction of benzaldehyde with three substrates (malononitrile, ethyl cyanoacetate, and cyano-acetic acid *tert*-butyl ester). Reprinted with permission from [101]. Copyright (2007) American Chemical Society. 27
1.17 Structural illustration of NU-1000. Reprinted by permission from Macmillan Publishers Ltd: Nature Communications [112], Copyright (2015). 28
1.18 Molecular representation of MIL-53. (a) BDC linkers are coordinated to M-OH-M-OH chains. (b) Each zigzag chain is connected with four neighboring chains. (c) Narrow pore phase. (d) Large pore phase. Reprinted with permission from [116]. Copyright (2017) American Chemical Society. 29

3.1 (a) Schematic illustration of $Zr_6O_4(OH)_4$ octahedra containing twelve carboxylate groups coordinated to the zirconium cations (top) and 2-X-1,4-benzenedicarboxylate (BDC-X) organic struts, X=H, NH_2 or SO_3H (bottom). (b) The structural representation of cubic unit cell of UiO-66. Zr, blue; O, red; C, gray; H, white. 56
3.2 FT-IR spectra of UiO-66 and its analogues. 57
3.3 PXRD patterns of experimental UiO-66-X (X=H, NH_2, and SO_3H) and simulated UiO-66. 58
3.4 Yield of 5-HMF in the catalytic conversion of glucose to 5-HMF. Conditions: Microwave, 100 mg glucose, 10 mg UiO-66-X (X=H, NH_2, SO_3H), 2 mL DMSO-*d6*, 160 °C, 20 min. 59

3.5 Nitrogen gas adsorption isotherms at 77 K of UiO-66-X and MOF 808. 60
3.6 Effect of reaction time on yield of 5-HMF. Reaction conditions: Microwave, 100 mg glucose, 10 mg UiO-66, 2 mL DMSO-*d6*, 160 °C. . . 62
3.7 Pathways for decomposition of 5-HMF during glucose conversion. . . 63
3.8 Effect of temperature on yield of 5-HMF. Conditions: Microwave, 100 mg glucose, 10 mg UiO-66, 2 mL DMSO-*d6*, 30 min. 64
3.9 Recycling experiment of UiO-66. Conditions: Microwave, 1000 mg glucose, 200 mg UiO-66, 15 mL DMSO-*d6*, 160 °C, 30 min. 66
3.10 Colour on the right is due to the humin formation. 68
3.11 Nitrogen gas adsorption isotherms at 77 K of UiO-66 and UiO-66-humin. 69
3.12 PXRD patterns of UiO-66 simulated (black), UiO-66 synthesized (red), and UiO-66-humin (blue). 71
3.13 FT-IR spectra of UiO-66 and UiO-66-humin. 72
3.14 ^{13}C solid-state NMR spectrums of UiO-66 (bottom) and UiO-66-humin (top). 73
3.15 (a) Illustration of $Zr_6O_4(OH)_4$ secondary building units (top) and trimesic acid (H_3BTC) organic linkers (bottom). (b) Structural representation of MOF 808. Zr, blue; O, red; C, gray; H, white. μ_3-O and H atoms are omitted for clarity. 75
3.16 FT-IR spectra of MOF 808. 76
3.17 PXRD patterns of simulated and synthesized MOF 808. 77
3.18 FT-IR spectra of MOF 808 and MOF 808-humin. 78
3.19 FT-IR spectra of UiO-66-humin and MOF 808-humin. 79

List of Abbreviations and Symbols

ACS	American Chemical Society
Al	aluminium
$AlCl_3$	aluminium chloride
Al_2O_3	aluminium oxide
aq.	aqueous
ATR	attenuated total reflectance
Au	gold
bdc	1,4-benzenedicarboxylate
BDC-SO_3Na	monosodium 2-sulfoterephthalate
BHMF	2,5-bis(hydroxymethyl)furan
BHMTHF	2,5-bis(hydroxymethyl)tetrahydrofuran
[BMIM][Cl]	1-butyl-3-methylimidazolium chloride
bpb	1,4-bis(4′-pyrazolyl) benzene
bpdc	4,4′-biphenyldicarboxylate
bpy	bipyridine
btapa	benzene tricarboxylic acid tris[*N*-(4-pyridyl)amide]
btc	1,3,5-benzenetricarboxylate
Br	bromine
C	carbon

Cd	cadmium
ChCl	choline chloride
cm	centimeter
Co	cobalt
CO_2	carbon dioxide
$CrCl_2$	chromium(II) chloride
$CrCl_3$	chromium(III) chloride
Cu	copper
$CuCl_2$	copper(II) chloride
DEF	diethylformamide
DFF	2,5-diformylfuran
DMA	dimethylacetamide
DMF	dimethylformamide
DMSO	dimethyl sulfoxide
DOE	Department of Energy
[EMIM][Cl]	1-ethyl-3-methylimidazolium chloride
equiv.	equivalent
FA	formic acid
FDA	2,5-furandicarboxylic acid
FT-IR	Fourier-transform infrared spectroscopy
GHG	greenhouse gas
h	hour
H_2	hydrogen
H_3BTC	trimesic acid
HCl	hydrochloric acid
HCS	hollow carbon sphere

HMF	hydroxymethylfurfural
HMFCA	5-hydroxymethyl-2-furancarboxylic acid
H_2O	water
HPLC	high-performance liquid chromatography
hr	hour
H_2SO_4	sulfuric acid
HT	hydrotalcite
IPA	isopropanol
K	kelvin
kHz	kilohertz
KOH	potassium hydroxide
kV	kilovolt
L	liter
M	metal
mA	milliampere
MAS	magic-angle spinning
mg	milligram
Mg	magnesium
MHz	megahertz
MIBK	methyl isobutyl ketone
MIL	Materials of Institut Lavoisier
μL	microliter
mL	milliliter
mm	millimeter
mM	millimolar
mmHg	millimeter of mercury

mmol	millimole
mol	mole
MOF	metal-organic framework
N_2	nitrogen
NaCl	sodium chloride
NaOH	sodium hydroxide
Nb_2O_5	niobium oxide
NH_2	amino group
NMP	1-methyl-2-pyrrolidinone
NMR	nuclear magnetic resonance
NUS	National University of Singapore
O	oxygen
OH	hydroxyl group
Pd	palladium
PEF	polyethylene furanoate
PET	polyethylene terephthalate
POST	Pohang University of Science and Technology
Pt	platinum
PXRD	powder X-ray diffraction
pymo	hydroxypyrimidinolate
ref.	reference
Rh	rhodium
Ru	ruthenium
s	second
S	sulfur
Sn-Mont	tin montmorillonite

SO_3H	sulfonic acid
teda	triethylenediamine
Temp	temperature
TEMPO	(2,2,6,6-tetramethylpiperidin-1-yl)oxyl
TMS	tetramethylsilane
TOF	turn over frequency
UiO	Universitetet i Oslo
U.S.	United States of America
v	volume
V	volts
wt	percentage by weight
Zn	zinc
Zr	zirconium
$ZrCl_4$	zirconium(IV) chloride
$ZrOCl_2{\cdot}8H_2O$	zirconium(IV) oxychloride octahydrate
ZSM	Zeolite Socony Mobil

Chapter 1

Introduction

1.1 Biomass Feedstocks

Biomass refers to all organic materials which can be produced by plants via photosynthesis. [1, 2] Photosynthesis is a carbon fixation process yielding carbon-rich compounds by reduction of carbon dioxide in the air, water, and sunlight. [3] Biomass can store solar energy in the chemical bonds of their structures, which can be converted to valuable products such as biodiesel, biogas, and bioethanol. [1]

There are several driving forces raising interest in biomass conversion, both industrially and academically, in recent years. The main driving force is an environmental issue. Production of greenhouse gases (GHG) (mainly CO_2) from the combustion of fossil fuels, which causes the rise in atmospheric levels of CO_2, contributes to climate change. [4, 5] Another issue is that current petroleum production might not satisfy demand for fuel or chemical supply. [5, 6] Biomass development and research is also driven by (i) the occurrence of advanced technologies related to biomass conversion which could lower the cost of production; [1] (ii) the promotion of renewable resources and the funding provided by governments in Europe or the United States which could

be beneficial for the development of biomass; [5] (iii) increasing market demand for bio-based materials or chemicals. [5]

The main components of biomass are cellulose, hemicellulose, and lignin. [1, 7] Generally, cellulose, hemicellulose, and lignin comprise 40-60, 20-40, and 10-25 wt.% of biomass respectively. [1,7,8] Cellulose is a linear chain of glucose polymer, consisting of (1,4)-D-glucopyranose linear repeating units, in which the units are linked through the oxygen covalently bonded to C1 of one glucose unit and C4 of the adjoining ring. (Figure 1.1). [1, 9]

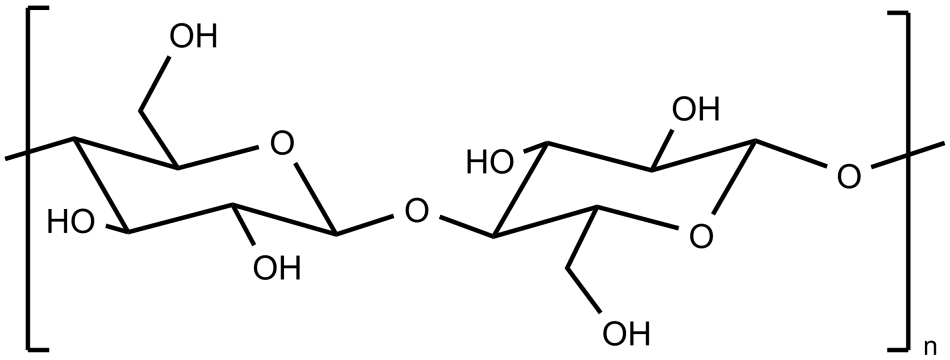

Figure 1.1: Single repeating unit of cellulose.

Cellulose is used to make clothes or build houses in the form of cotton or wood, and can yield paper through chemical and mechanical approaches. [10] Moreover, pulp fibers extracted from cellulose could be converted to nanocelluloses via different chemical and mechanical processes. [9,10] Nanocelluloses have a wide range of applications such as enhancement of fiber bond strength in paper materials, flavour carriers, and suspension stabilizers in food products as well as fracturing fluid in oil recovery.

Hemicellulose is a heterogeneous polymer, composed of pentoses (xylose, arabinose), hexoses (glucose, mannose, galactose), and sugar acids (Figure 1.2). [1, 11] Typically, the average molecular weight of hemicellulose is less than 30,000. [1, 11] Unlike cellulose, hemicellulose is an amorphous, random polymer containing branches

while cellulose has a crystalline structure without branches. Due to the amorphous structure, hemicellulose can be more soluble compared to cellulose.

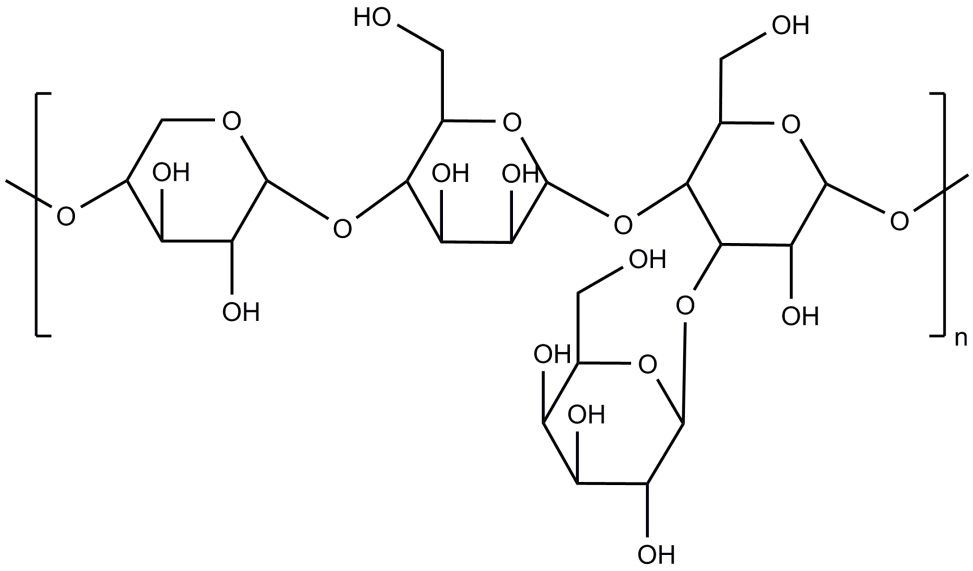

Figure 1.2: Structure of hemicellulose.

Hemicellulose is the second largest component of the lignocellulosic biomass. Although studies on applications of hemicellulose are not as common as those of celluloses, hemicellulose still possesses some valuable applications, for example, raw material for biological medicine, [12] production of renewable petroleum refinery feedstock, [13] and conversion to hydrogels. [14]

Lignin is a potential renewable source of aromatic compounds and is a polymer with a backbone containing benzene rings attached to a 3 carbon chains, named phenyl-propanes. [1] In nature, lignin can be formed through an enzyme initiated dehydrogenative polymerization of three different precursors with zero, one or two methoxyl groups attached to the rings (Figure 1.3). [1, 15] Lignin is a large, cross-linked chemical compound derived from wood and is an important component of the cell walls of plants. In the plant cell, lignin is more hydrophobic than cellulose and hemicellulose so it can inhibit the absorption of water by polysaccharides and

thus conduct water in the plant stem by allowing the water into the vascular tissues. Moreover, lignin can act as a defensive barrier against attack by insects, keeping plants healthy.

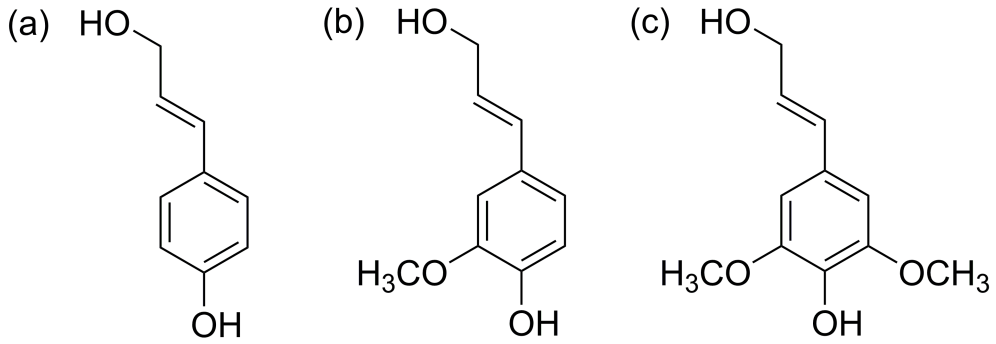

Figure 1.3: Structures of three lignin precursors: (a) *p*-coumaryl alcohol; (b) coniferyl alcohol; (c) sinapyl alcohol.

Lignin can be a good natural adsorbent. It can adsorb not only metal ions (Cu^{2+}, Pd^{2+}, Zn^{2+}), but also materials such as dyes, pesticides, and surfactants. [15] Lignin is an important resource for fuels like chars and aromatic chemicals. [16] More importantly, lignin can be used as a raw material for hydrogels instead of synthetic polymers because of its biocompatible and biodegradable properties. [17]

Biomass is the fourth largest utilized energy source around the world after coal, oil, and natural gas. [18] Biomass feedstocks are diverse and biorenewable materials, which can be utilized directly or converted to other forms of fuel products. There are typically six major categories of biomass feedstocks as shown in Figure 1.4. These include forest, crops, alcohol fuels, garbage, aquatic plants, and landfill gas.

Forest and agricultural waste products are the most widely used feedstocks, which can generate electricity. For industry and timber/agricultural companies, this is a win-win solution. In industry, less carbon but more clean energy is produced. In forestry and agriculture, using waste to generate electricity can save disposal costs. Solid waste like garbage is another alternative to generating energy. Approximately 2,000

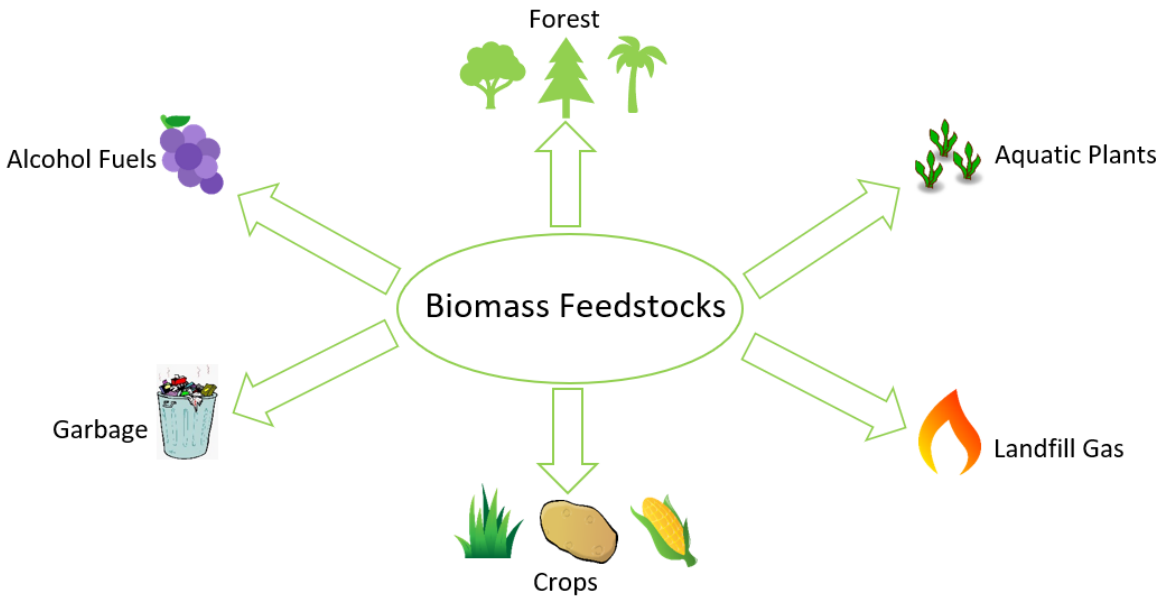

Figure 1.4: The schematic illustration of categories of biomass.

pounds of garbage produces as much heat energy as 500 pounds of coal. However, we should be aware that not all garbage is biomass feedstock. Plastics manufactured from petroleum or natural gas are not considered biomass. The main advantage of using garbage as a renewable resource is diverting garbage from landfills. Furthermore, burying garbage in landfills directly can cause severe environmental issues like air and water pollution. Alcohol fuels, which are typically made from corn, grain or some other plant waste, are prospective feedstocks. Ethanol is the most common feedstock among alcohol fuels. Ethanol-based biofuels can replace fossil fuels as the preferred fuel for cars and power engines and are the main transportation fuel in Brazil. There are several advantages of ethanol fuel. For one, fuel efficiency is improved if ethanol is used alone or as an additive because the oxygen content of the fuel is increased. Also, ethanol-based fuel burns cleaner than traditional fossil fuels.

Landfill gas is another source of renewable energy. In nature, bacteria and fungi decompose dead plants and animals, causing them to rot. This decomposition process

might take a long time to finish, but, during this period, methane gas is produced. Landfill gas consists of around 50% methane and 50% CO_2 along with a trace amount of non-methane organic compounds. [19] Landfill gas is a greenhouse gas in itself and will contribute to climate change if it escapes into the atmosphere. However, if landfill gas could be captured and utilized, then it will not only produce valuable chemicals, but it will reduce the emissions into the atmosphere.

Aquatic plants are an ideal biomass resource due to fast growth rates and tolerance of various environmental conditions. [20] Among aquatic plants, microalgae are a good choice to replace fossil fuels since the oils from microalgae are a good substitute for fossil fuels. The main contributor to climate change is excess CO_2 emission into the atmosphere through fossil fuel combustion. Interestingly, for microalgae growth, CO_2 can be consumed because CO_2 is the major nutrient. [20] If power plants collaborate with microalgae farmers to purify CO_2 from burning fossil fuels, then CO_2 emissions could be reduced. [20] Also, microalgae itself can be used as a raw material for biofuel.

Overall, biomass feedstocks play an important role in reducing atmospheric CO_2. The ultimate goal of biomass utilization is to reduce global warming and resolve the air pollution issue.

1.2 5-Hydroxymethylfurfural (5-HMF) and Its Applications

Fossil fuel is still the main resource of energy and chemical production. However, with the rise in oil prices and the concern about environmental issues, it is necessary to explore alternative resources to replace fossil fuel. Biomass is a viable alternative since it is a renewable resource. Among various primary renewable platform chemicals, 5-hydroxymethylfurfural (5-HMF) is considered as an important building block

due to its abundance and availability from carbohydrates, for instance, glucose, fructose, sucrose, and cellulose. [21] Moreover, 5-HMF still retains all six carbon atoms from hexoses and high selectivity can be obtained from hexoses, especially from fructose. [22] 5-HMF is considered as a biobased product from carbohydrates in the U.S. Department of Energy (DOE) "Top 10+4" list of biobased chemicals. [23, 24]

5-HMF is a heterocyclic organic compound containing aldehyde and alcohol functional groups in the 2,5 positions of a furan ring. [25] 5-HMF can be an important intermediate for a broad range of compounds such as adipic acid (monomer of nylon), 2,5-furandicarboxylic acid, and *p*-xylene (via 2,5-dimethylfuran). [21, 25] The latter two chemical compounds can be further converted to other potential products including fuel additives and the biobased polymer polyethylene furanoate (PEF) that is a possible alternative to the petroleum-derived polymer polyethylene terephthalate (PET) (Figure 1.5). [26]

5-HMF was first reported by Dull *et al.* in 1895 and was synthesized by heating inulin and oxalic acid solution under pressure. [21, 27] In the same year, Kiermeyer reported another approach to synthesize 5-HMF using sugar cane as the starting material. [21, 28] Over the next few years, many chemists reported their syntheses of 5-HMF. Middendorp published detailed research on the synthesis and characterization of 5-HMF. [29, 30] The first review of 5-HMF was published in 1951 by Newth. [31] In 1973, Feather and Harris reported the mechanisms of dehydration reactions of carbohydrates in both acidic and basic conditions. [32] Around twenty years later, a review focusing on the manufacture of 5-HMF was reported by Kuster. [33] In 2001, a detailed review was published by Lewkowski, describing the synthesis and applications of 5-HMF and its derivatives. [29] Recently, several reviews regarding 5-HMF production and characterization were published. A critical review of 5-HMF as an important building block was published by Afonso *et al.* in 2011. [21] Zhang *et*

al. reported the past, present, and future of 5-HMF production, which gave a general overview of 5-HMF production from bioresources. [34]

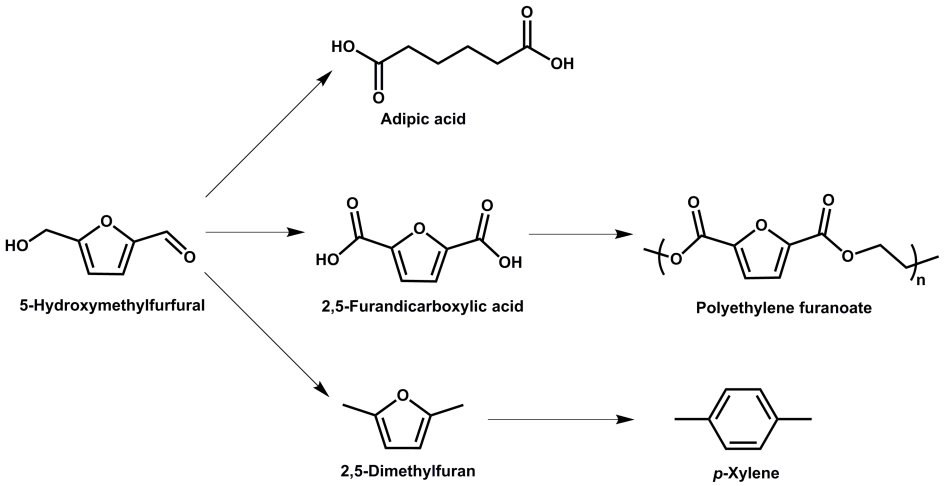

Figure 1.5: Applications of 5-HMF as a building block.

Generally, 5-HMF is synthesized by the acid-catalyzed dehydration of carbohydrates like fructose or glucose. The reaction conditions include several parameters such as temperature, reaction time, solvents, substrate concentration, and catalyst system. The most common classification of the synthesis of 5-HMF is by catalyst types. Herein, the dehydration reaction is divided into two major categories based on the catalysis mechanism: homogeneous catalysis and heterogeneous catalysis.

(1) Homogeneous catalytic dehydration reaction

The first class of homogeneous catalysts in the dehydration of carbohydrates to 5-HMF are mineral and organic acids, for instance, hydrochloric acid, sulfuric acid, and maleic acid. Shanks *et al.* reported a systematic study comparing different homogeneous mineral and organic acids in the dehydration of monosaccharides. [35] In the dehydration of fructose, they found that proton acidity was the major factor of the conversion rates while associated anions had a minor effect on the selectivity of 5-HMF. [35] Hansen *et al.* conducted a microwave-assisted reaction of fructose to 5-HMF using HCl as the catalyst in water. [36] In their work, the yield of 5-HMF

was 53% with microwaving at 200 °C for 1 min (Table 1, entry 1). [36] Water is an environmentally friendly solvent due to non-toxicity and low cost. However, the selectivity for 5-HMF is relatively poor with water as the solvent. Moreover, extraction of 5-HMF from the aqueous phase is difficult since 5-HMF is water-soluble. [37] In the dehydration of fructose, Zhang *et al.* reported an 85% yield of 5-HMF using HCl as the catalyst in the solvent mixture of IPA/water (v/v=97:3) at 120 °C for 3 h (Table 1, entry 2). [38] Ionic liquids are a common solvent in the homogeneous catalysis of carbohydrates. Ionic liquids, which usually refer to organic salts in the liquid state, can dissolve carbohydrates effectively. [39, 40] Fairly high yield (85%) of 5-HMF can be obtained from fructose using H_2SO_4 as the catalyst in [BMIM][Cl] at 120 °C for 4 h (Table 1, entry 3). [41] Ordonez and co-workers reported only 6% yield of 5-HMF in the dehydration of glucose using HCl at 110 °C for 4 h (Table 1, entry 5). [42] In general, for the dehydration of glucose to 5-HMF, the first mechanistic step is the isomerization of glucose to fructose followed by conversion to 5-HMF. [43] Mineral acids cannot catalyze the dehydration of glucose effectively due to the absence of Lewis acidic catalyst in the transformation of glucose to fructose. [44]

Lewis acidic metal chlorides such as $AlCl_3$, $CrCl_2$ and $CrCl_3$ are another important class of homogeneous catalysts. Saha *et al.* found 70% yield of 5-HMF could be obtained using $AlCl_3$ in the dehydration of fructose (Table 1, entry 4). [45] However, glucose is more attractive as the biomass feedstock due to its low cost. [49] In the dehydration of glucose, Konig and co-workers obtained a 45% yield of 5-HMF in ChCl using $CrCl_2$ at 110 °C for 3 min (Table 1, entry 6). [46] They also reported a 62% yield of 5-HMF using sucrose as the substrate (Table 1, entry 8). [46] Zhang's group reported a combination of $CrCl_2$ and [EMIM][Cl] to give higher yields (68-70%) of 5-HMF (Table 1, entry 7). [47] The presence of $CrCl_2$ can enable the dehydration of glucose to 5-HMF via a two-step process (isomerization of glucose to fructose followed

Table 1.1: Conversion of carbohydrates to 5-HMF using homogeneous catalysts

		Reaction Conditions				
Entry (ref.)	Substrate	Solvent	Catalyst	Temp (°C)	Time	5-HMF yield (%)
1 [36]	Fructose (27 wt%)	water	HCl	200	1 min	53
2 [38]	Fructose (1 mmol)	97:3(v/v) IPA/water	HCl	120	3 h	85
3 [41]	Fructose	[BMIM][Cl]	H_2SO_4	120	4 h	85
4 [45]	Fructose (5 wt%)	DMSO	$AlCl_3$	140	5 min	70
5 [42]	Glucose (18 wt%)	water	HCl	110	4 h	6
6 [46]	Glucose	6:4(wt/wt) ChCl/Glucose	$CrCl_2$	110	3 min	45
7 [47]	Glucose (10 wt%)	[EMIM][Cl]	$CrCl_2$	100	3 h	68-70
8 [46]	Sucrose	5:5 (wt/wt) ChCl/Sucrose	$CrCl_2$	100	1 h	62
9 [48]	Cellulose (10 wt%)	[EMIM][Cl]	$CrCl_3$	140	10 min	36
10 [48]	Cellulose (10 wt%)	[EMIM][Cl]	$CrCl_3/CuCl_2$	140	5 min	40

by conversion to 5-HMF). [47, 50] The possible mechanism of isomerization of glucose to fructose starts with the ring-opening of glucose and then two oxygen atoms coordinate to hexacoordinate chromium(II) compound to form the putative enediolate intermediate. [48, 50] Compared to glucose and fructose, cellulose is a very promising feed due to its abundance and easy availability from nonfood resources. [50, 51] Dehydration of cellulose using mineral or organic acids is difficult due to uncontrolled side reactions producing levulinic and formic acid. Steele *et al.* showed that $CrCl_3$ afforded 36% yield of 5-HMF from cellulose (Table 1, entry 9). [48]. Also, 40% yield of 5-HMF could be attained with a more selective catalyst system combining $CrCl_3$ and $CuCl_2$ (Table 1, entry 10). [48]

(2) Heterogeneous catalytic dehydration reaction

The main drawback of homogeneous catalysts are difficulties in catalyst separation and recycling. [52] Therefore, a variety of heterogeneous solid acid catalysts, including ion-exchange resins, zeolites, and metal-organic frameworks, have been developed and investigated in recent years.

Ion-exchange resins are a group of insoluble materials with high molecular weight that act as the medium for exchange of ions. The most common ion-exchange resins are Amberlyst® and Dow type resins, which show high catalytic activity in the dehydration of fructose to 5-HMF. [53] Dumesic and Chheda studied the conversion of fructose and its precursors (inulin and sucrose) using an ion-exchange resin in the presence of biphasic systems and achieved nearly 83% yield of 5-HMF from fructose using a in the biphasic mixture of H_2O-NMP(w/w=4:6)/MIBK (Table 2, entry 1). [54] Under the identical conditions, conversion of inulin gave a slightly lower yield (69%) of 5-HMF, which was due to hydrolysis of glycosidic bonds (Table 2, entry 2). [54] Furthermore, only 43% yield of 5-HMF was formed in the dehydration of sucrose since half of sucrose is composed of glucose molecules that did not react under the condi-

tions explored. (Table 2, entry 3). [54] Satsuma *et al.* demonstrated two approaches to increase the yield of 5-HMF. [55] One is water removal from the reaction mixture under evacuation at 0.97 $\times 10^5$ Pa and another is to decrease the particle size of Amberlyst-15. [55] In the dehydration of fructose using Amberlyst-15, the 92% yield of 5-HMF obtained under evacuation (Table 2, entry 4) was 16% higher than that without evacuation (Table 2, entry 5) since water removal could prevent undesired byproducts formation and drive the reaction forward. [55] Powdered Amberlyst-15-P with diameters in the range of 0.15-0.053 mm (Table 2, entry 6 and 7) gave a higher 5-HMF yield than the Amberlyst-15 (0.71-0.50 mm) (Table 2, entry 4 and 5) either under evacuation or without evacuation. [55] This was likely due to the higher surface area of the catalyst.

In 2009, Takagaki *et al.* demonstrated the dehydration of glucose to 5-HMF by a simple one-pot reaction route using a solid acid/base catalyst system. [56] In their study, [56] Mg-Al hydrotalcite (HT) was chosen as the solid base catalyst for glucose isomerization to fructose and Amberlyst-15 was used in the acid-catalyzed dehydration of fructose to 5-HMF. They found that the presence of the base was a critical factor in the dehydration of glucose: without HT, no 5-HMF was obtained (Table 2, entry 8) while the yield increased to 42% using a combination of HT/Amberlyst-15 (Table 2, entry 9). [56] When sucrose was selected as the substrate, a higher yield of 5-HMF resulted (Table 2, entry 10). [56]

Zeolites are solid, microporous, aluminosilicate minerals, which can be naturally occurring or synthetic. Generally, the formula of zeolite is $M^n{}_{x/n}Si_{1-x}Al_xO_2 \cdot yH_2O$. Zeolites bear a formal negative charge and need cations to counterbalance the overall charge. [57] These cations (counter ions) are mobile and present in the pores and/or voids within the structure. Zeolites have an open framework built up from tetrahedra and their structure is usually periodic. Compared to homogeneous catalysts, zeolites

Table 1.2: Conversion of carbohydrates to 5-HMF using heterogeneous catalysts

		Reaction Conditions				
Entry (ref.)	Substrate	Solvent	Catalyst	Temp (°C)	Time	5-HMF yield (%)
1 [54]	Fructose (10 wt%)	4:6 water-NMP/MIBK	resin	90	18 h	83
2 [54]	Inulin (10 wt%)	4:6 water-NMP/MIBK	resin	90	21 h	69
3 [54]	Sucrose (10 wt%)	5:5 water-NMP/MIBK	resin	90	21 h	43
4 [55]	Fructose (1.7 mmol)	DMSO	Amberlyst-15	120	2 h	92
5 [55]	Fructose (1.7 mmol)	DMSO	Amberlyst-15	120	2 h	76
6 [55]	Fructose (1.7 mmol)	DMSO	Amberlyst-15-P	120	2 h	100
7 [55]	Fructose (1.7 mmol)	DMSO	Amberlyst-15-P	120	2 h	100
8 [56]	Glucose (0.56 mmol)	DMF	Amberlyst-15	100	3 h	0
9 [56]	Glucose (0.56 mmol)	DMF	HT/Amberlyst-15	80	9 h	42
10 [56]	Sucrose (0.29 mmol)	DMF	HT/Amberlyst-15	120	3 h	54
11[58]	Sucrose (0.11 mol)	3:1(v/v) MIBK/water	zeolite mordenite	165	400 min	49
12[59]	Glucose (5 wt%)	7:3(v/v) THF:DMSO	Sn-Mont	160	3 h	53.5
13[60]	Glucose (0.83 mmol)	7:3(v/v) MIBK/NaCl aq. phase	H-ZSM-5	195	30 min	42
14[61]	Glucose (0.83 mmol)	7:3(v/v) MIBK/NaCl aq. phase	H-Beta	195	30 min	56
15[62]	Cellulose (2.5 wt%)	water	Bimodal-HZ-5	190	4 h	46

are easier to separate from reaction mixtures. Moreover, zeolites are more thermally stable in aqueous systems compared to ion-exchange resins. [58] Nijhuis *et al.* studied the dehydration of fructose to 5-HMF over zeolites and reported 49% yield of 5-HMF using zeolite mordenite (Table 2, entry 11). [59] In 2012, Wang's group first reported conversion of glucose to 5-HMF using a Sn-Mont catalyst. [60] Under the optimal reaction conditions, high yield (53.5%) of 5-HMF with 98.4% conversion could be achieved (Table 2, entry 12) and the catalyst was still stable after six runs. [60] Recently, Maireles-Torres *et al.* showed H-ZSM-5 could enable the catalytic conversion of glucose to 5-HMF with 80% glucose conversion and 42% 5-HMF yield (Table 2, entry 13). [61] In 2017, the same group reported their latest results of acid-catalyzed dehydration of glucose to 5-HMF using zeolites. [62] They demonstrated a higher yield (56%) of 5-HMF was obtained using the H-Beta zeolite in NaCl aqueous solution/MIBK at 195 °C after 30 min (Table 2, entry 14). Bokade and co-workers developed a bimodal-HZ-5 zeolite from post-synthesis modification of H-ZSM-5. [63] They found this modified heterogeneous catalyst provided up to a 46% 5-HMF yield with 67% cellulose conversion (Table 2, entry 15). [63]

Another class of heterogeneous catalysts are metal-organic frameworks (MOFs). A more detailed discussion of carbohydrate conversion to 5-HMF using MOFs is presented in Section 1.4.

In the above paragraphs, properties and synthesis of 5-HMF are presented and discussed in detail. Additionally, synthetic applications of 5-HMF are an important part of HMF chemistry and lots of papers related to this research theme have been published. In general, synthetic applications of 5-HMF can be divided into two categories (oxidation reactions and reduction reactions).

(1) Oxidation of 5-HMF

Oxidation reactions can occur on the formyl group to form 5-hydroxymethyl-

2-furancarboxylic acid (HMFCA) or the hydroxyl group to form 2,5-diformylfuran (DFF) or both groups to form 2,5-furandicarboxylic acid (FDA) (Figure 1.6). It is worth mentioning that FDA was also included by the U.S. Department of Energy (DOE) in the "Top 10+4" list of biobased chemicals for being an important chemical building block. [23, 24]

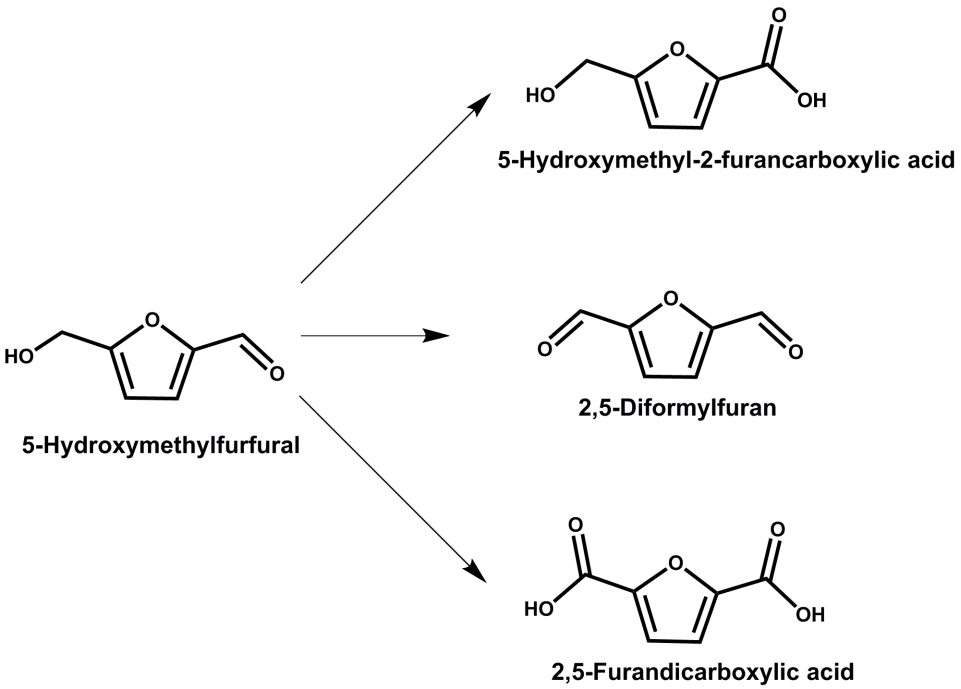

Figure 1.6: Three products from oxidation of 5-HMF.

FDA can be synthesized by oxidation of both formyl and hydroxyl groups of 5-HMF. Morikawa reported oxidation of 5-HMF to FDA using either nitrogen tetroxide or nitric acid in DMSO. [21, 64] El-Hajj *et al.* [65] and Cottier *et al.* [66] showed the oxidation of 5-HMF using nitric acid. However, these nitrogen-containing compounds are not environmental benign oxidants. Several authors attempted the oxidation of 5-HMF to FDA with metal catalysts. The first study of the oxidation of 5-HMF to FDA with noble metals was reported by Vinke *et al.* in 1991. [67] Based on their results, [67] different metals (Pd, Pt, Ru) supported on different carriers were tested

in the oxidation catalysis but only Pt supported on Al_2O_3 (Pt/Al_2O_3) gave nearly quantitative yield of FDA using a partial oxygen pressure of 0.2 in the basic aqueous solution at 60 °C. Further discussion of the conversion of 5-HMF to FDA is beyond the scope of this thesis.

(2) Reduction of 5-HMF.

2,5-Bis(hydroxymethyl)furan (BHMF) (Figure 1.7), which is formed during the reduction reaction of the formyl group of 5-HMF, is an important building block with several applications in the preparation of polymers and polyurethane foams. [22, 68] Moreover, 2,5-Bis(hydroxymethyl)furan (BHMF) can be used in the production of crown ethers. [69] Additionally, further transformation of 2,5-bis(hydroxymethyl)furan (BHMF) leads to 2,5-bis(hydroxymethyl)tetrahydrofuran (BHMTHF), which is also an important building block with various applications, for instance, solvent, [70], monomer, [68], the precursor for producing other high-valued chemical cmpounds such as 1,6-hexanediol (Figure 1.7). [71, 72]

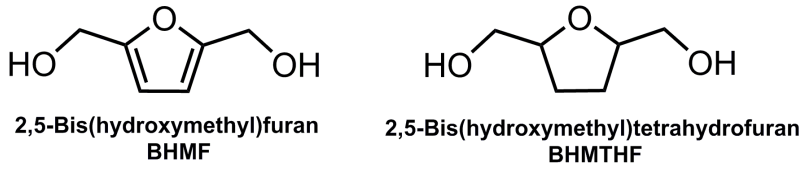

Figure 1.7: Two products of reduction of the formyl group of 5-HMF.

Reduction of both formyl and hydroxyl groups of 5-HMF produces 2,5-dimethylfuran (Figure 1.8), which can be used as the biofuel since its energy density is 40% higher than that of ethanol, making it comparable with gasoline. [73]

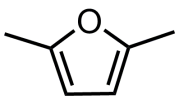

Figure 1.8: Molecular structure of 2,5-dimethylfuran.

Dumesic *et al.* [73] described a two-step synthetic pathway for the preparation of

2,5-dimethylfuran. 5-HMF was extracted using a biphasic system and hydrogenated using a carbon-supported copper/ruthenium (Cu-Ru/C) catalyst, thereby producing 71% of 2,5-dimethylfuran. [73] In 2010, Chidambaram and Bell studied the catalytic activity of different carbon-supported metal (Pd, Pt, Ru and Rh) catalysts in [EMIM][Cl] under hydrogen pressure in the hydrogenation of 5-HMF and found the best yield (15%) with 47% conversion of 5-HMF using Pd/C catalyst at 120 °C for 1 h. [74] Compared with the catalytic system in 1-butanol and THF, such low yield and conversion is due to the lower temperature and less reaction time as well as poor solubility of H_2 in [EMIM][Cl]. [74]

To sum up, the use of 5-HMF as the platform chemical is of particular importance and would gain much more attention in the future because 5-HMF can be obtained from cheap and environmentally-friendly biomass resources that can reduce or replace the use of petroleum-based chemicals, thereby decreasing air or water pollution.

1.3 Metal-Organic Frameworks (MOFs) Introduction

Metal-organic frameworks (MOFs) are a class of crystalline materials, built up from metal cations/clusters (nodes) and bridging organic ligands (linkers), in which multivalent aromatic carboxylic acids or nitrogen-containing aromatic compounds assemble with metal elements such as zinc, copper, zirconium and chromium to form 3D frameworks (Figure 1.9). [75–78] With various choices of node and linker, MOFs having a wide range of pore-sizes and pore functionalities have been formed. [75, 79] Additionally, pre- and post-synthetic functionalization of MOFs can introduce different linkers or functionalities into the frameworks. [80, 81] The combination of the facile synthesis as well as large pore size, high surface area, low density and thermal and

chemical stability have made these porous materials ideal in many different fields, for instance, gas storage and separation, [82, 83] catalysis, [81, 84] proton- and ion- conduction. [85, 86] Among various applications, catalysis is one of the earliest proposed and demonstrated applications for MOFs. [87,88] Herein, the role of MOFs in the field of catalysis is presented and discussed.

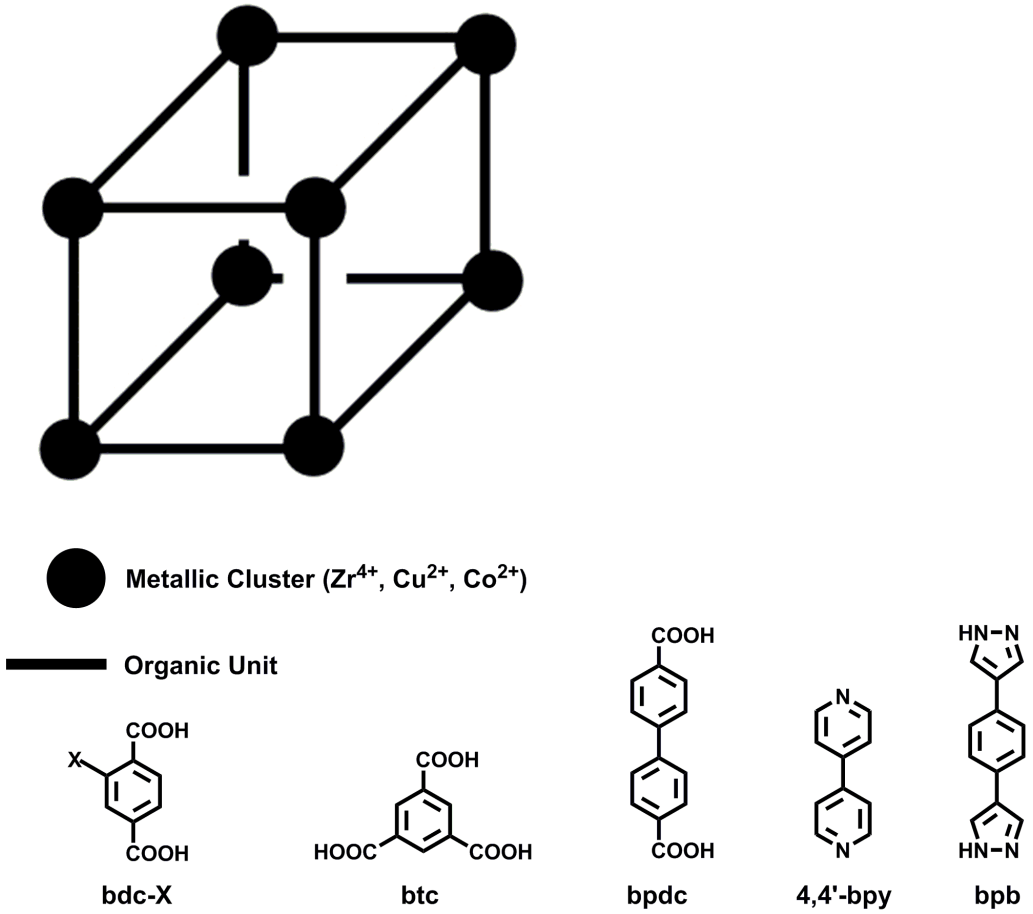

Figure 1.9: Schematic illustration of metal-organic frameworks (MOFs).

In general, the condition for MOF synthesis should be met so that metal-ligand bonds can be formed, broken and reformed to allow for structure propagation. [89] Moreover, dynamic bonds are critical to the growth of crystalline and ordered materials in order to correct any erroneous bonding. [89] Until now, several synthetic methods have been published in the literature such as mechanochemistry, electro-

chemistry, microwave-assisted heating, sonochemistry, hydrothermal, solvothermal, and so on (Figure 1.10). Currently, among these different methods, the most widely used approach to synthesize MOFs is solvothermal synthesis, where MOF crystals usually grow in a pure solvent or a solvent mixture after heating to high temperatures. Typically, this approach requires mixing a metal salt with a multitopic organic component in a high boiling point solvent (e.g. DMF, DMA, DEF) in a screw-top glass vial or Teflon-lined stainless steel bomb. [89] After full dissolution, the mixture is heated either in an oven or on a hot plate equipped with nonflammable silicone-based oil bath in a fumehood. [89] Small variations of reaction parameters (temperature, time and pH) dramatically affect the crystal size, structure and purity.

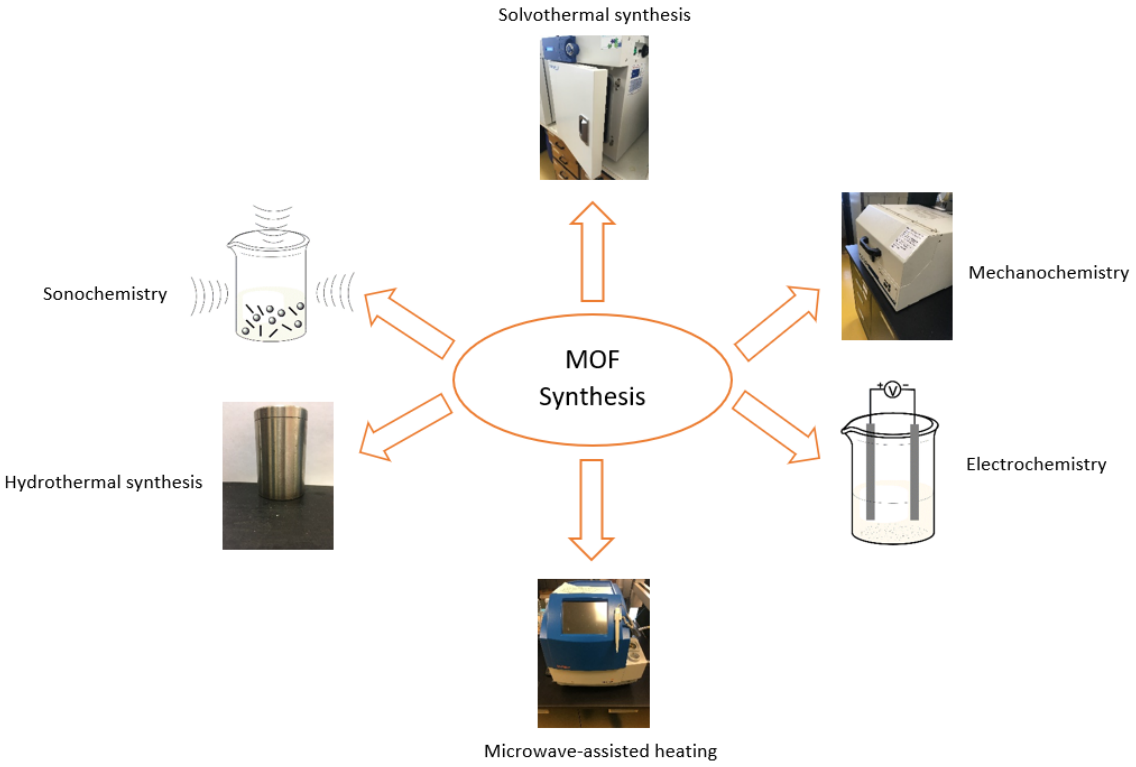

Figure 1.10: Graphical illustration of different approaches to MOF synthesis

In some cases, the addition of a modulator can inhibit rapid precipitation of amor-

phous or crystalline materials. [89,90] Modulators, which are nonstructural and monotopic compounds such as benzoic acid, acetic acid and hydrochloric acid, can form dynamic bonds with the metal salt, thereby slowing down the formation of structural bonds by competing with the organic linkers for metal coordination sites. [89] In particular, modulators are commonly used in the synthsis of zirconium-containing metal-organic frameworks (Zr-MOFs). Katz *et al.* reported a reproducible HCl-containing synthesis of UiO-66, UiO-67, and their corresponding derivatives. They concluded that the use of HCl does not only accelerate the synthesis but also promotes formation of hexa-Zr clusters prior to linker binding. [91] Schaate *et al.* described that the use of acetic acid and benzoic acid modulators can slow down the reaction, affording highly crystalline products or single crystals. [92]

Zeolites, which are commonly used commercial catalysts, have some similarities with MOFs such as large surface area, uniformly sized pores and cavities, but they still have differences. For example, MOFs are more tunable than zeolites due to the presence of organic functional groups in MOF structures. [81] Also, though MOFs can tolerate high temperatures and some are stable above 500 °C, [93] zeolites show extraordinary thermal stability. This means that MOFs cannot compete with zeolites for reactions under harsh conditions, especially high temperature. Instead, MOFs are more suitable in high-value-added reactions (e.g. fine chemical production, individual enantiomer reaction and delicate molecule preparation) under milder conditions. [81] Smaller pore size characteristic of zeolites inhibits the catalytic reaction of large molecules, for instance, polyaromatics, carbohydrates and glycerides. [80] Therefore, while MOF-based catalysis is still in its infancy, MOFs are a good alternative for catalytic reactions due to the diverse structures that can be accessed.

Taking into account the above, MOFs could be potential coordination polymers for catalysis. However, the literature focusing on catalysis with MOFs is limited so far

due to two aspects: (1) the inferior chemical and thermal stability of MOFs compared with zeolites; (2) the presence of organic linkers that can have adverse effects on catalytic activity of MOFs since the coordination sphere of the metals is blocked by organic struts. [94, 95] To address the latter disadvantage, introduction of labile ligands (usually solvent molecules) can result in unsaturated metal sites once these labile ligands are removed during the activation process. Herein, several publications will be presented and exciting results of using MOFs as catalysts will be discussed. [95] In general, MOF-based catalysis can be divided into three categories: (1) catalysis with metal active nodes; (2) catalysis with organic ligands; and (3) MOFs as host matrices or nanometric reaction cavities. [95]

(1) Catalysis with metal active nodes

In the synthesis of metal active nodes, the catalytic reaction takes place on the metal nodes, either as isolated metal centers [95] or as clusters [96], chains [97], or sheets [98], connected with the organic struts.

In 2007, Llabrés i Xamena *et al.* demonstrated that aerobic alcohol oxidation, olefin hydrogenation and Suzuki C-C coupling could be actively catalyzed by using a Pd-containing MOF with a formula of $[Pd(2\text{-pymo})_2]_n$ (2-pymo = 2-hydroxypyrimidinolate). [94] Expansion of the Pd coordination sphere without the collapse of the structural framework coupled with the insensitivity to moisture, allowed the MOF to participate in catalysis. Moreover, the shape- and size- properties of the Pd-MOF indicated that the heterogeneous catalytic reactions took place inside the MOF. [94] In Suzuki cross coupling, they reported 99% selectivity toward the desired cross-coupling product with 85% conversion using Pd-MOF at 150 °C after 5 h. [94] Further examples of catalysis at metal-centres in MOFs will be described below in the section on 5-HMF formation using MOFs.

In 2009, Zhang, Llabrés i Xamena and Corma prepared a Au(III)-containing MOF

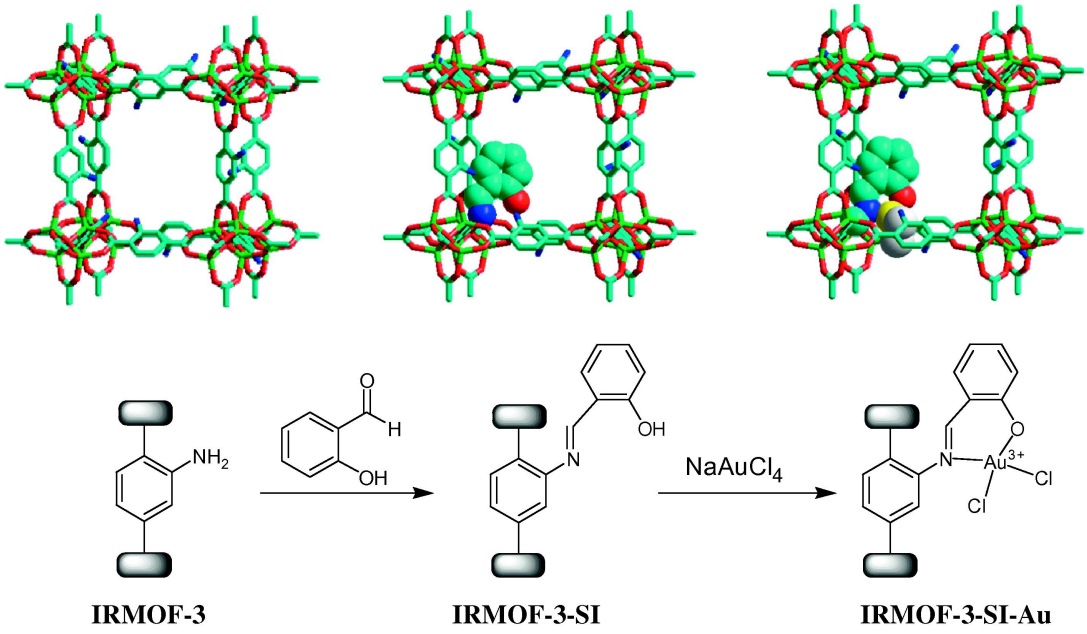

Figure 1.11: Two-step modification process for producing Au(III)-MOF. Zn, green; O, red; C, light blue; N, deep blue; Au, yellow; Cl, white. H atoms are omitted for clarity. Reprinted from [99], Copyright (2009), with permission from Elsevier.

by a covalent post-synthesis approach. [99] The material was synthesized via a two-step process shown in Figure 1.11. This Au(III)-containing MOF was modified from the starting material IRMOF-3 ($Zn_4O(BDC\text{-}NH_2)_3$), by reacting the amino groups with salicylaldehyde to form the corresponding salicylideneimine, followed by reacting with a suitable gold precursor, $NaAuCl_4$, to generate the Au(III)-containing MOF. [99] Owing to the presence of accessible isolated Au(III) active sites, they hypothesized that this modified Au(III)-MOF could be a possible alternative to the common Au(III) salt catalyst. [99] Based on their study on the hydrogenation of 1,3-butadiene, [99] the Au-MOF was used as the catalyst and Au/TiO_2 catalysts were applied for comparison. They found that nearly 100% conversion was obtained using the Au(III)-MOF as compared with fairly lower conversion (ca. 9%) produced by Au/TiO_2 catalysts. Moreover, the TOF calculated for Au-MOF was 540 h^{-1}, which was much higher than the values calculated for Au/TiO_2 (50.4 h^{-1}). [99]

(2) Catalysis with organic ligands

This class of catalysis depends on the functional groups of the organic ligands to enable catalytic reaction. [95] However, not all organic ligands are catalytically-active unless they possess two different types of functional groups: coordinative groups, L_1, which are needed for building up the MOF framework through coordination to the metal nodes, and reactive groups, L_2, which are able to catalyze the reaction (Figure 1.12). [95] This requirement limits the number of MOFs that belong to this class since these reactive groups should be free and available to reach the catalytic substrates and not be coordinated to the metal nodes. [95] Thus, it is difficult to prepare this class of MOF.

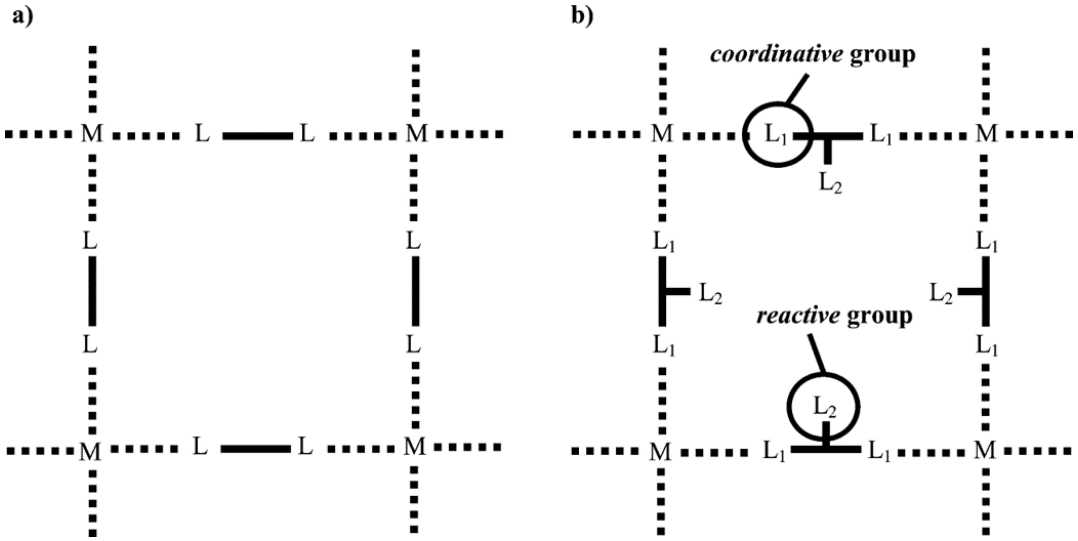

Figure 1.12: Schematic illustration of (a) a "Classic" MOF with only coordinative groups (L) and (b) a MOF having both coordinative (L_1) and reactive (L_2) groups. Reprinted with permission from [95]. Copyright (2010) American Chemical Society.

In 2000, Kim *et al.* [100] first prepared a MOF (referred to as POST-1) containing reactive functional groups. POST-1 was obtained by reaction between Zn^{2+} ions and the enantiopure chiral organic building block (synthesized from D- or L-tartaric acid) containing a carboxylic acid and a pyridine group (Figure 1.13). This homochiral open-framework consisted of $[Zn_3(\mu^3\text{-O})]$ units, in which each Zn^{2+} ion

was connected with the central μ^3-O, four oxygen atoms from four carboxylic ligands bridging two Zn^{2+} ions and a nitrogen atom on pyridine from a neighbouring trimer (Figure 1.13). [95] This structure contained 6 pyridyl groups per trimer: three of them were coordinative groups that linked to three Zn^{2+} metal cations from another three trimers while the other three were free and available for catalytic reactions. [95]

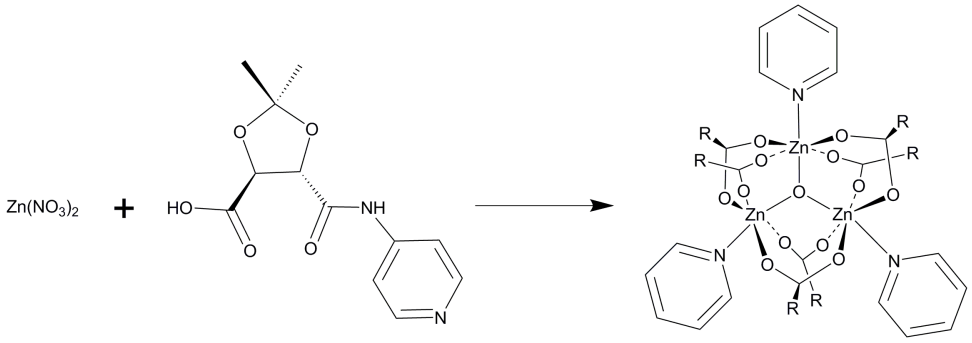

Figure 1.13: Equation for preparation of the POST-1 homochiral MOF (CO_2R = organic carboxylate anions).

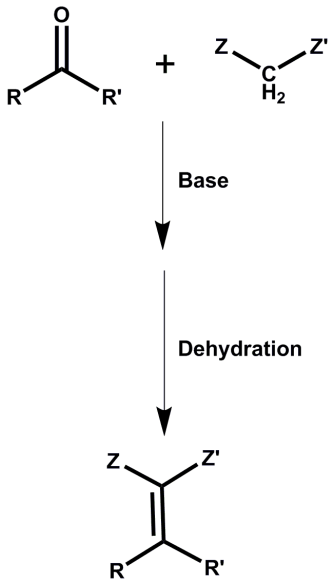

Figure 1.14: Schematic illustration of the Knoevenagel condensation reaction.

Kitagawa *et al.* performed the Knoevenagel condensation reaction using a 3D coordination solid catalyst. [101] The Knoevenagel condensation is a nucleophilic addition

between an aldehyde or ketone, and an active hydrogen compound (diethyl malonate, ethyl acetoacetate, nitromethane etc.) followed by spontaneous dehydration producing an unsaturated product (Figure 1.14). [102] Based on their description, [101] they developed a MOF with the formula $[Cd(4\text{-btapa})_2(NO_3)_2]\cdot 6H_2O\cdot 2DMF$ (4-btapa = 1,3,5-benzene tricarboxylic acid tris[*N*-(4-pyridyl)amide], containing three amide groups which are responsible for the catalytic activity, and three pyridyl groups coordinating to Cd^{2+} ions (Figure 1.15). Furthermore, they used this MOF in the Knoevenagel condensation reactions of benzaldehyde with three different active methylene compounds: malononitrile, ethyl cyanoacetate, and cyano-acetic acid *tert*-butyl ester (Figure 1.16). They found that extremely high conversion (98%) was obtained using malononitrile as the substrate while the other two gave negligible conversion, thereby indicating the reaction occurred inside the pores of the MOF and not on the surface since malononitrile had the smallest size (4.5×6.9 Å) and could enter the pores (4.7×7.3 Å) of the MOF. [101] However, compared with the pore size of the MOF, other two substrates had much greater size (4.5×10.3 Å for ethyl cyanoacetate and 5.8×10.3 Å for cyano-acetic acid *tert*-butyl ester), which prevented them entering into the pores and accessing the catalytic sites. [101]

(3) MOFs as host matrices or nanometric reaction cavities

MOFs do not need to directly participate in a catalytic reaction. MOFs can act as the physical space where the reaction occurs or a cavity where the catalytic centers are encapsulated. [95] The pores of MOFs can be used to encapsulate different varieties of substances, such as metal or metal oxide nanoparticles. Notably, encapsulating species into MOFs have several advantages like better stability, higher dispersion, controlled size, or even suppression of self-deactivation, as compared with the same species in the solution. [103]

Sometimes the enclosed space of MOFs has significant impact on the product

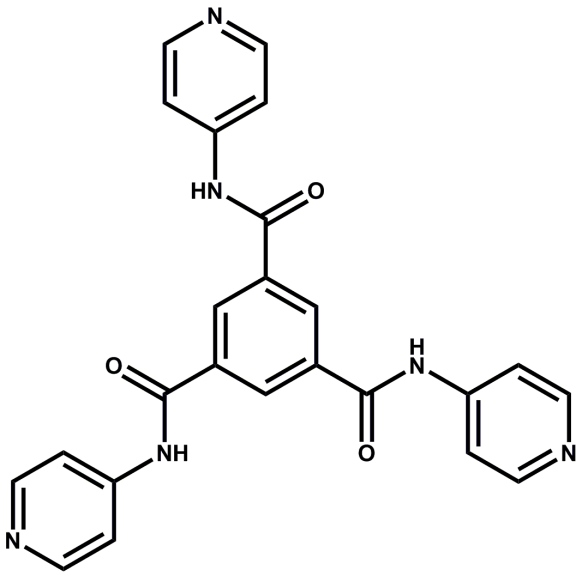

Figure 1.15: The structure of 4-btapa.

selectivity. This happens when the substrate or product as well as the MOF matrix have similar dimensions. [103] A clear example of this is styrene polymerization inside the channels of a MOF. When the catalytic radical reaction occurred inside the pores of MOFs with the general formula of $[M_2(bdc)_2(teda)]$ (M: Zn^{2+} or Cu^{2+}, teda = triethylenediamine), Endo *et al.* noticed that the recovered polymer had a extremely low polydispersity (1.66) after MOF dissolution. [104] Conversely when the similar polymerization reaction was performed without the presence of the MOF, a high polydispersity of 4.68 was observed. [104] More interestingly, EPR spectroscopy of the polymerization of styrene in the MOF gave an intense signal belonging to the propagating living radical, and this signal still showed up even after storing the sample for one week at 70 °C. They proposed that this was suppression of the termination reaction and radical transfer in the channels of MOFs. [104]

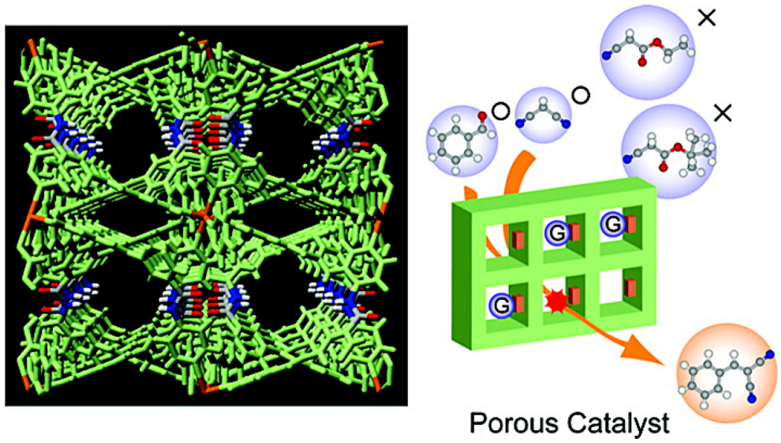

Figure 1.16: Illustration of Knoevenagel condensation reaction of benzaldehyde with three substrates (malononitrile, ethyl cyanoacetate, and cyano-acetic acid *tert*-butyl ester). Reprinted with permission from [101]. Copyright (2007) American Chemical Society.

1.4 Catalytic Conversion of Carbohydrates to 5-HMF using MOFs

Homogeneous and heterogeneous catalysis of carbohydrates to 5-HMF have been discussed in Section 1.2. To narrow the scope towards the present thesis, the catalytic conversion of carbohydrates to 5-HMF using MOFs will be discussed in this section. Due to several advantages of MOFs as mentioned in the last section, MOFs have recently been considered as heterogeneous catalysts for the dehydration of carbohydrates to 5-HMF. [105]

In 2011, the first example of a MOF (MIL-101) in a dehydration of fructose and glucose to 5-HMF was described by Hensen *et al.*, but the yield was only 2% with glucose. [106] Kitagawa *et al.* investigated the isomerization of glucose to fructose using different MIL-101(Cr) derivatives (with BDC-NH_2, -NO_2 and -SO_3H) in water and found that MIL-101(Cr)-SO_3H afforded higher conversion (21.6%) to fructose. [107] Bao *et al.* obtained high yield (44.9%) of 5-HMF from glucose with 45.8% selectivity using MIL-101(Cr)-SO_3H. [108] A 29% yield of 5-HMF was reported by Herbst and

Janiak using MIL-101(Cr)-SO_3H in a THF/H_2O (v:v=39:1) solvent mixture. [109]

Very recently, Katz, Farha and co-workers [110] reported that phosphate-modification of NU-1000 enabled the dehydration of glucose to 5-HMF. NU-1000 consists of $Zr_6(\mu_3\text{-O})_4(\mu_3\text{-OH})_4(OH)_4(OH_2)_4$ nodes, where eight of twelve octahedral edges are coordinated to TBAPy organic linkers (H_4TBAPy = 1,3,6,8-tetrakis(*p*-benzoic-acid)pyrene) (Figure 1.17). [111] Although unmodified NU-1000 gave 60% glucose conversion, which is much higher than 16% conversion of the control reaction without catalyst, only 2.3% 5-HMF yield was obtained with bare NU-1000. [110] After phosphate-modification of NU-1000, the yield of 5-HMF increased to 15% with PO_4/NU(half) as the catalyst (PO_4/NU(half) means the amount of phosphoric acid used in the modification is half-equimolar to OH groups of NU-1000). Under the optimal reaction conditions (1 mM glucose loading, 9:1 (v/v) 2-PrOH/water, 413 K, 7 h), the highest yield (64%) of 5-HMF was achieved. [110]

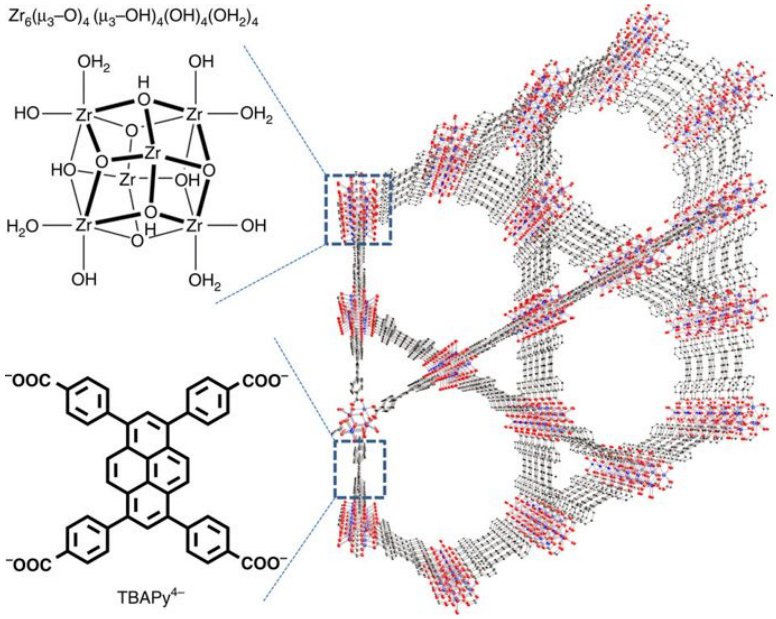

Figure 1.17: Structural illustration of NU-1000. Reprinted by permission from Macmillan Publishers Ltd: Nature Communications [112], Copyright (2015).

Zhao's research group developed a new MOF, NUS-6, built up from zirconium

(Zr) or hafnium (Hf) clusters and sulfonated organic linkers. [113] They applied these catalysts in the dehydration of fructose to 5-HMF and achieved high yields (98%) and selectivity (98%) using NUS-6(Hf). [113] However, it should be mentioned that they performed these reactions in DMSO and it is known that DMSO itself can catalyze fructose conversion to 5-HMF. [114]

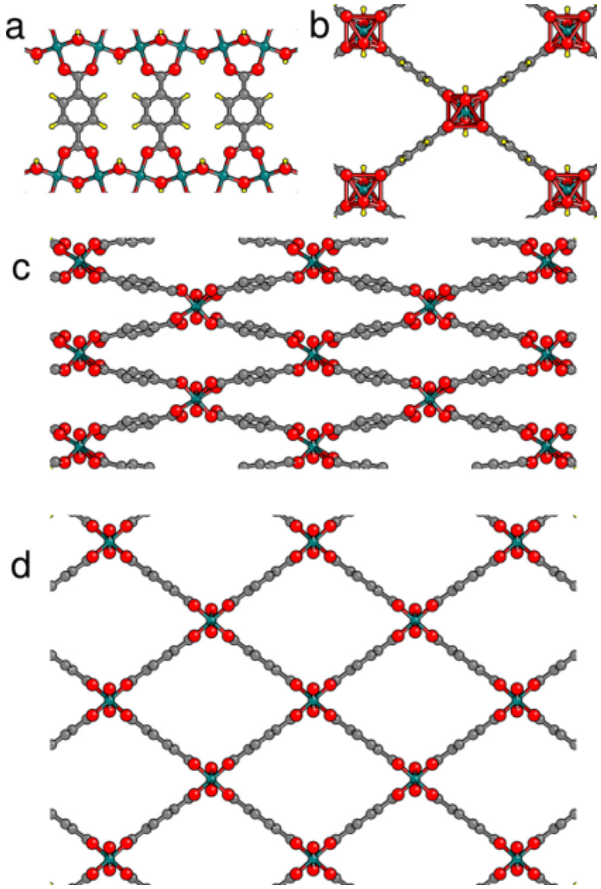

Figure 1.18: Molecular representation of MIL-53. (a) BDC linkers are coordinated to M-OH-M-OH chains. (b) Each zigzag chain is connected with four neighboring chains. (c) Narrow pore phase. (d) Large pore phase. Reprinted with permission from [116]. Copyright (2017) American Chemical Society.

Wang *et al.* used bare MIL-53(Al) in the conversion of carboxymethyl cellulose (CMC) to 5-HMF in the aqueous phase. [115] The general formula of MIL-53 is $M(OH)(C_8H_4O_4)$, where M refers to a trivalent species, for instance, Cr, Sc, Al, Ga, and Fe. [116, 117] These structures are built from zigzag M-OH-M-OH chains,

cross-linked by 1,4-benzodicarboxylate organic struts (Figure 1.18). [116] Each M is coordinated to two OH units and four carboxylate oxygens, producing the octahedral coordination unit. [116] Wang and co-workers reported the maximum yield (40.3%) of 5-HMF using MIL-53(Al) with only water as solvent at 473 K for 4 h, and was able to reuse MIL-53(Al) three times without loss in catalytic activity. [115]

To summarize, heterogeneous catalysts attract considerable attention owing to the desire for easy separation and re-use. Among various heterogeneous catalysts, MOFs show superiority due to their Lewis acidity, diverse pre- and post-functionalization, and large surface area.

1.5 Summary

Given increasing atmospheric CO_2 levels resulting in part from the combustion of fossil fuels, it is important to explore renewable energy alternatives to either reduce the need for fossilized resources, or completely replace them. Biomass, mainly composed of cellulose, hemicellulose and lignin, is considered a renewable alternative.

5-HMF, an important platform chemical, can be derived from different carbohydrates such as glucose, fructose, sucrose, and cellulose via dehydration reactions using homogeneous or heterogeneous catalysts. One unavoidable limitation of homogeneous catalysts is the difficulty in post-reaction catalyst separation and recycling. Thus, in the past few years, several kinds of heterogeneous catalysts have been developed for this transformation.

For my research, glucose was chosen as the substrate due to its lower cost and its accessibility directly from cellulose. MOFs are the primary catalyst applied here due to their unique properties and promising catalytic activities in the limited number of studies reported so far. Herein, a series of Zr-cluster-based MOFs were prepared,

characterized and investigated in the dehydration reaction of glucose to 5-HMF. Experimental details and discussion will be presented in Chapter 2 and 3.

References

[1] Peter McKendry. Energy production from biomass (part 1): overview of biomass. *Bioresource Technology*, 83(1):37 – 46, 2002.

[2] Lopamudra Devi, Krzysztof J Ptasinski, and Frans J.J.G Janssen. A review of the primary measures for tar elimination in biomass gasification processes. *Biomass and Bioenergy*, 24(2):125 – 140, 2003.

[3] Howard Gest. History of the word photosynthesis and evolution of its definition. *Photosynthesis Research*, 73(1):7–10, 2002.

[4] Juan Carlos Serrano-Ruiz, Ryan M. West, and James A. Dumesic. Catalytic Conversion of Renewable Biomass Resources to Fuels and Chemicals. *Annual Review of Chemical and Biomolecular Engineering*, 1(1):79–100, 2010.

[5] Pierre Gallezot. Conversion of biomass to selected chemical products. *Chemical Society Reviews*, 41:1538–1558, 2012.

[6] Avelino Corma, Sara Iborra, and Alexandra Velty. Chemical Routes for the Transformation of Biomass into Chemicals. *Chemical Reviews*, 107(6):2411–2502, 2007.

[7] Haiping Yang, Rong Yan, Hanping Chen, Dong Ho Lee, and Chuguang Zheng. Characteristics of hemicellulose, cellulose and lignin pyrolysis. *Fuel*, 86(12):1781 – 1788, 2007.

[8] Lili Lin, Rong Yan, Yongqiang Liu, and Wenju Jiang. In-depth investigation of enzymatic hydrolysis of biomass wastes based on three major components: Cellulose, hemicellulose and lignin. *Bioresource Technology*, 101(21):8217 – 8223, 2010.

[9] Robert J. Moon, Ashlie Martini, John Nairn, John Simonsen, and Jeff Youngblood. Cellulose nanomaterials review: structure, properties and nanocomposites. *Chemical Society Reviews*, 40:3941–3994, 2011.

[10] Nathan Grishkewich, Nishil Mohammed, Juntao Tang, and Kam Chiu Tam. Recent advances in the application of cellulose nanocrystals. *Current Opinion in Colloid & Interface Science*, 29:32 – 45, 2017.

[11] Badal C. Saha. Hemicellulose bioconversion. *Journal of Industrial Microbiology and Biotechnology*, 30(5):279–291, 2003.

[12] Jing Bian, Feng Peng, Xiao-Peng Peng, Pai Peng, Feng Xu, and Run-Cang Sun. Structural features and antioxidant activity of xylooligosaccharides enzymatically produced from sugarcane bagasse. *Bioresource Technology*, 127:236 – 241, 2013.

[13] Hakan Olcay, Ayyagari V. Subrahmanyam, Rong Xing, Jason Lajoie, James A. Dumesic, and George W. Huber. Production of renewable petroleum refinery diesel and jet fuel feedstocks from hemicellulose sugar streams. *Energy & Environmental Science*, 6:205–216, 2013.

[14] Muzaffer Ahmet Karaaslan, Mandla A. Tshabalala, Daniel J. Yelle, and Gisela Buschle-Diller. Nanoreinforced biocompatible hydrogels from wood hemicelluloses and cellulose whiskers. *Carbohydrate Polymers*, 86(1):192 – 201, 2011.

[15] Suhas, P.J.M. Carrott, and M.M.L. Ribeiro Carrott. Lignin – from natural adsorbent to activated carbon: A review. *Bioresource Technology*, 98(12):2301 – 2312, 2007.

[16] Pooya Azadi, Oliver R. Inderwildi, Ramin Farnood, and David A. King. Liquid fuels, hydrogen and chemicals from lignin: A critical review. *Renewable and Sustainable Energy Reviews*, 21:506 – 523, 2013.

[17] Vijay Kumar Thakur and Manju Kumari Thakur. Recent advances in green hydrogels from lignin: a review. *International Journal of Biological Macromolecules*, 72:834 – 847, 2015.

[18] Rakesh C. Saxena, Dilip K. Adhikari, and Hari B. Goyal. Biomass-based energy fuel through biochemical routes: A review. *Renewable and Sustainable Energy Reviews*, 13(1):167 – 178, 2009.

[19] Shaobin Wang, G. Q. (Max) Lu, and Graeme J. Millar. Carbon Dioxide Reforming of Methane To Produce Synthesis Gas over Metal-Supported Catalysts: State of the Art. *Energy & Fuels*, 10(4):896–904, 1996.

[20] Lewis M. Brown and Kathryn G. Zeiler. Aquatic biomass and carbon dioxide trapping. *Energy Conversion and Management*, 34(9):1005 – 1013, 1993.

[21] Andreia A. Rosatella, Svilen P. Simeonov, Raquel F. M. Frade, and Carlos A. M. Afonso. 5-Hydroxymethylfurfural (HMF) as a building block platform: Biological properties, synthesis and synthetic applications. *Green Chemistry*, 13:754–793, 2011.

[22] Robert-Jan van Putten, Jan C. van der Waal, Ed de Jong, Carolus B. Rasrendra, Hero J. Heeres, and Johannes G. de Vries. Hydroxymethylfurfural, A

Versatile Platform Chemical Made from Renewable Resources. *Chemical Reviews*, 113(3):1499–1597, 2013.

[23] Joseph J. Bozell and Gene R. Petersen. Technology development for the production of biobased products from biorefinery carbohydrates-the US Department of Energy's "Top 10" revisited. *Green Chemistry*, 12:539–554, 2010.

[24] Todd Werpy, Gene Petersen, Andy Aden, Joe Bozell, John Holladay, James White, Amy Manheim, D. Eliot, L. Lasure, and Susanne Jones. Top Value Added Chemicals From Biomass. Volume 1 - Results of Screening for Potential Candidates From Sugars and Synthesis Gas. Department of Energy Washington DC. 2004.

[25] Tianfu Wang, Michael W. Nolte, and Brent H. Shanks. Catalytic dehydration of C6 carbohydrates for the production of hydroxymethylfurfural (HMF) as a versatile platform chemical. *Green Chemistry*, 16:548–572, 2014.

[26] Aloysius J. J. E. Eerhart, André P. C. Faaij, and Martin K. Patel. Replacing fossil based PET with biobased PEF; process analysis, energy and GHG balance. *Energy & Environmental Science*, 5:6407–6422, 2012.

[27] Georg Düll. Action of oxalic acid on inulin. *Chemiker Zeitung*, 19:216–220, 1895.

[28] Joseph Kiermayer. A derivative of furfuraldehyde from laevulose. *Chemiker Zeitung*, 19:1003–1005, 1895.

[29] Jarosław Lewkowski. Synthesis, chemistry and applications of 5-hydroxymethylfurfural and its derivatives. *Arkivoc*, 2001:17–54, 2001.

[30] Joan A. Middendorp. Sur l'oxymethylfurfurol. *Recueil des Travaux Chimiques des Pays-Bas*, 38(1):1–71, 1919.

[31] Frederick H. Newth. The Formation of Furan Compounds from Hexoses. *Advances in Carbohydrate Chemistry*, 6:83 – 106, 1951.

[32] Milton S. Feather and John F. Harris. Dehydration Reactions of Carbohydrates Issued as Journal Paper No. 6502 of the Missouri Agricultural Experiment Station, Columbia, Mo. *Advances in Carbohydrate Chemistry and Biochemistry*, 28:161 – 224, 1973.

[33] Ben F. M. Kuster. 5-Hydroxymethylfurfural (HMF). A Review Focussing on its Manufacture. *Starch - Stärke*, 42(8):314–321, 1990.

[34] Siew Ping Teong, Guangshun Yi, and Yugen Zhang. Hydroxymethylfurfural production from bioresources: past, present and future. *Green Chemistry*, 16:2015–2026, 2014.

[35] Basak Cinlar, Tianfu Wang, and Brent H. Shanks. Kinetics of monosaccharide conversion in the presence of homogeneous Bronsted acids. *Applied Catalysis A: General*, 450:237 – 242, 2013.

[36] Thomas S. Hansen, John M. Woodley, and Anders Riisager. Efficient microwave-assisted synthesis of 5-hydroxymethylfurfural from concentrated aqueous fructose. *Carbohydrate Research*, 344(18):2568 – 2572, 2009.

[37] Takashi Okano, Kun Qiao, Quanxi Bao, Daisuke Tomida, Hisahiro Hagiwara, and Chiaki Yokoyama. Dehydration of fructose to 5-hydroxymethylfurfural (HMF) in an aqueous acetonitrile biphasic system in the presence of acidic ionic liquids. *Applied Catalysis A: General*, 451:1 – 5, 2013.

[38] Guangshun Yi, Siew Ping Teong, Xiukai Li, and Yugen Zhang. Purification of Biomass-Derived 5-Hydroxymethylfurfural and Its Catalytic Conversion to 2,5-Furandicarboxylic Acid. *ChemSusChem*, 7(8):2131–2135, 2014.

[39] Furong Tao, Huanling Song, and Lingjun Chou. Dehydration of fructose into 5-hydroxymethylfurfural in acidic ionic liquids. *RSC Advances*, 1:672–676, 2011.

[40] Richard P. Swatloski, Scott K. Spear, John D. Holbrey, and Robin D. Rogers. Dissolution of Cellose with Ionic Liquids. *Journal of the American Chemical Society*, 124(18):4974–4975, 2002.

[41] Carsten Sievers, Ildar Musin, Teresita Marzialetti, Mariefel B. Valenzuela Olarte, Pradeep K. Agrawal, and Christopher W. Jones. Acid-Catalyzed Conversion of Sugars and Furfurals in an Ionic-Liquid Phase. *ChemSusChem*, 2(7):665–671, 2009.

[42] Diego Garcés, Eva Díaz, and Salvador Ordóñez. Aqueous Phase Conversion of Hexoses into 5-Hydroxymethylfurfural and Levulinic Acid in the Presence of Hydrochloric Acid: Mechanism and Kinetics. *Industrial & Engineering Chemistry Research*, 56(18):5221–5230, 2017.

[43] Chaochao Yue, Guanna Li, Evgeny A. Pidko, Jan J. Wiesfeld, Marcello Rigutto, and Emiel J. M. Hensen. Dehydration of Glucose to 5-Hydroxymethylfurfural Using Nb-doped Tungstite. *ChemSusChem*, 9(17):2421–2429, 2016.

[44] Mika Ohara, Atsushi Takagaki, Shun Nishimura, and Kohki Ebitani. Syntheses of 5-hydroxymethylfurfural and levoglucosan by selective dehydration of glucose using solid acid and base catalysts. *Applied Catalysis A: General*, 383(1):149 – 155, 2010.

[45] Sudipta De, Saikat Dutta, and Basudeb Saha. Microwave assisted conversion of carbohydrates and biopolymers to 5-hydroxymethylfurfural with aluminium chloride catalyst in water. *Green Chemistry*, 13:2859–2868, 2011.

[46] Florian Ilgen, Denise Ott, Dana Kralisch, Christian Reil, Agnes Palmberger, and Burkhard Konig. Conversion of carbohydrates into 5-hydroxymethylfurfural in highly concentrated low melting mixtures. *Green Chemistry*, 11:1948–1954, 2009.

[47] Haibo Zhao, Johnathan E. Holladay, Heather Brown, and Z. Conrad Zhang. Metal Chlorides in Ionic Liquid Solvents Convert Sugars to 5-Hydroxymethylfurfural. *Science*, 316(5831):1597–1600, 2007.

[48] Hussein Abou-Yousef, El Barbary Hassan, and Philip Steele. Rapid conversion of cellulose to 5-hydroxymethylfurfural using single and combined metal chloride catalysts in ionic liquid. *Journal of Fuel Chemistry and Technology*, 41(2):214 – 222, 2013.

[49] Ana I. Torres, Michael Tsapatsis, and Prodromos Daoutidis. Biomass to chemicals: Design of an extractive-reaction process for the production of 5-hydroxymethylfurfural. *Computers & Chemical Engineering*, 42:130 – 137, 2012.

[50] Joseph B. Binder and Ronald T. Raines. Simple Chemical Transformation of Lignocellulosic Biomass into Furans for Fuels and Chemicals. *Journal of the American Chemical Society*, 131(5):1979–1985, 2009.

[51] Arthur J. Ragauskas, Charlotte K. Williams, Brian H. Davison, George Britovsek, John Cairney, Charles A. Eckert, William J. Frederick, Jason P. Hallett, David J. Leak, Charles L. Liotta, Jonathan R. Mielenz, Richard Murphy,

Richard Templer, and Timothy Tschaplinski. The Path Forward for Biofuels and Biomaterials. *Science*, 311(5760):484–489, 2006.

[52] Basudeb Saha and Mahdi M. Abu-Omar. Advances in 5-hydroxymethylfurfural production from biomass in biphasic solvents. *Green Chemistry*, 16:24–38, 2014.

[53] Xinhua Qi, Masaru Watanabe, Taku M. Aida, and Richard Lee Smith, Jr. Catalytic dehydration of fructose into 5-hydroxymethylfurfural by ion-exchange resin in mixed-aqueous system by microwave heating. *Green Chemistry*, 10:799–805, 2008.

[54] Juben N. Chheda and James A. Dumesic. An overview of dehydration, aldol-condensation and hydrogenation processes for production of liquid alkanes from biomass-derived carbohydrates. *Catalysis Today*, 123(1):59 – 70, 2007.

[55] Ken ichi Shimizu, Rie Uozumi, and Atsushi Satsuma. Enhanced production of hydroxymethylfurfural from fructose with solid acid catalysts by simple water removal methods. *Catalysis Communications*, 10(14):1849 – 1853, 2009.

[56] Atsushi Takagaki, Mika Ohara, Shun Nishimura, and Kohki Ebitani. A one-pot reaction for biorefinery: combination of solid acid and base catalysts for direct production of 5-hydroxymethylfurfural from saccharides. *Chemical Communications*, pages 6276–6278, 2009.

[57] Christopher Rhodes. The Properties and Applications of Zeolites. *Science progress*, 93:223–84, 2010.

[58] Yunxiang Qiao, Nils Theyssen, and Zhenshan Hou. Acid-Catalyzed Dehydration of Fructose to 5-(Hydroxymethyl) furfural. *Recyclable Catalysis*, 2(1), 2015.

[59] Vitaly V. Ordomsky, John van der Schaaf, Jaap C. Schouten, and Tjeerd A. Nijhuis. The effect of solvent addition on fructose dehydration to 5-hydroxymethylfurfural in biphasic system over zeolites. *Journal of Catalysis*, 287:68 – 75, 2012.

[60] Jianjian Wang, Jiawen Ren, Xiaohui Liu, Jinxu Xi, Qineng Xia, Yanhong Zu, Guanzhong Lu, and Yanqin Wang. Direct conversion of carbohydrates to 5-hydroxymethylfurfural using Sn-Mont catalyst. *Green Chemistry*, 14:2506–2512, 2012.

[61] Mercedes Moreno-Recio, José Santamaría-González, and Pedro Maireles-Torres. Brönsted and Lewis acid ZSM-5 zeolites for the catalytic dehydration of glucose into 5-hydroxymethylfurfural. *Chemical Engineering Journal*, 303:22 – 30, 2016.

[62] Mercedes Moreno-Recio, Ignacio Jiménez-Morales, Pedro L. Arias, José Santamaría-González, and Pedro Maireles-Torres. The Key Role of Textural Properties of Aluminosilicates in the Acid-Catalysed Dehydration of Glucose into 5-Hydroxymethylfurfural. *ChemistrySelect*, 2(8):2444–2451, 2017.

[63] Kakasaheb Y. Nandiwale, Nitish D. Galande, Pratika Thakur, Sanjay D. Sawant, Vishal P. Zambre, and Vijay V. Bokade. One-Pot Synthesis of 5-Hydroxymethylfurfural by Cellulose Hydrolysis over Highly Active Bimodal Micro/Mesoporous H-ZSM-5 Catalyst. *ACS Sustainable Chemistry & Engineering*, 2(7):1928–1932, 2014.

[64] Shunichi Morikawa. Synthesis of 2,5-furandicarboxaldehyde from 5-hydroxymethylfurfural. *Noguchi Kenkyusho Jiho*, 22:20–27, 1979.

[65] Toni El Hajj, Antoine Masroua, Jean-Claude Martin, and Gérard Descotes. Synthesis of 5-hydroxymethylfuran-2-carboxaldehyde and its derivatives by acidic

treatment of sugars on ion-exchange resins. *Bulletin de la Societe Chimique de France*, (5):855–860, 1987.

[66] Louis Cottier, Gérard Descotes, Jaroslaw Lewkowski, and Romuald Skowroñski. ChemInform Abstract: Oxidation of 5-Hydroxymethylfurfural Under Sonochemical Conditions. *ChemInform*, 25(31), 1994.

[67] Peter Vinke, Wim van der Poel, and Herman van Bekkum. On the oxygen tolerance of noble metal catalysts in liquid phase alcohol oxidations the influence of the support on catalyst deactivation. *Studies in Surface Science and Catalysis*, 59:385 – 394, 1991.

[68] Claude Moreau, Mohamed Naceur Belgacem, and Alessandro Gandini. Recent Catalytic Advances in the Chemistry of Substituted Furans from Carbohydrates and in the Ensuing Polymers. *Topics in Catalysis*, 27(1):11–30, 2004.

[69] Joseph M. Timko and Donald J. Cram. Furanyl unit in host compounds. *Journal of the American Chemical Society*, 96(22):7159–7160, 1974.

[70] Alexandra J Sanborn and Paul D Bloom. Conversion of 2, 5-(hydroxymethyl) furaldehyde to industrial derivatives, purification of the derivatives, and industrial uses therefor, 2009. US Patent 7,579,490.

[71] Terrence J. Connolly, John L. Considine, Zhixian Ding, Brian Forsatz, Mellard N. Jennings, Michael F. MacEwan, Kevin M. McCoy, David W. Place, Archana Sharma, and Karen Sutherland. Efficient Synthesis of 8-Oxa-3-azabicyclo[3.2.1]octane Hydrochloride. *Organic Process Research & Development*, 14(2):459–465, 2010.

[72] Maya Chatterjee, Takayuki Ishizaka, and Hajime Kawanami. Selective hydrogenation of 5-hydroxymethylfurfural to 2,5-bis-(hydroxymethyl)furan using

Pt/MCM-41 in an aqueous medium: a simple approach. *Green Chemistry*, 16:4734–4739, 2014.

[73] Yuriy Román-Leshkov, Christopher J. Barrett, Zhen Y. Liu, and James A. Dumesic. Production of dimethylfuran for liquid fuels from biomass-derived carbohydrates. *Nature*, 447(7147):982, 2007.

[74] Mandan Chidambaram and Alexis T. Bell. A two-step approach for the catalytic conversion of glucose to 2,5-dimethylfuran in ionic liquids. *Green Chemistry*, 12:1253–1262, 2010.

[75] Yu-Ri Lee, Jun Kim, and Wha-Seung Ahn. Synthesis of metal-organic frameworks: A mini review. *Korean Journal of Chemical Engineering*, 30(9):1667–1680, 2013.

[76] Lauren E. Kreno, Kirsty Leong, Omar K. Farha, Mark Allendorf, Richard P. Van Duyne, and Joseph T. Hupp. Metal–Organic Framework Materials as Chemical Sensors. *Chemical Reviews*, 112(2):1105–1125, 2012.

[77] Michael O'Keeffe, Maxim A. Peskov, Stuart J. Ramsden, and Omar M. Yaghi. The Reticular Chemistry Structure Resource (RCSR) Database of, and Symbols for, Crystal Nets. *Accounts of Chemical Research*, 41(12):1782–1789, 2008.

[78] Christoph Janiak and Jana K. Vieth. MOFs, MILs and more: concepts, properties and applications for porous coordination networks (PCNs). *New Journal of Chemistry*, 34:2366–2388, 2010.

[79] Norbert Stock and Shyam Biswas. Synthesis of Metal-Organic Frameworks (MOFs): Routes to Various MOF Topologies, Morphologies, and Composites. *Chemical Reviews*, 112(2):933–969, 2012.

[80] David Farrusseng, Sonia Aguado, and Catherine Pinel. Metal–Organic Frameworks: Opportunities for Catalysis. *Angewandte Chemie International Edition*, 48(41):7502–7513, 2009.

[81] JeongYong Lee, Omar K. Farha, John Roberts, Karl A. Scheidt, SonBinh T. Nguyen, and Joseph T. Hupp. Metal-organic framework materials as catalysts. *Chemical Society Reviews*, 38:1450–1459, 2009.

[82] Julian Sculley, Daqiang Yuan, and Hong-Cai Zhou. The current status of hydrogen storage in metal-organic frameworks-updated. *Energy & Environmental Science*, 4:2721–2735, 2011.

[83] Youn-Sang Bae, Alexander M. Spokoyny, Omar K. Farha, Randall Q. Snurr, Joseph T. Hupp, and Chad A. Mirkin. Separation of gas mixtures using Co(II) carborane-based porous coordination polymers. *Chemical Communications*, 46:3478–3480, 2010.

[84] Chuan-De Wu, Aiguo Hu, Lin Zhang, and Wenbin Lin. A Homochiral Porous Metal−Organic Framework for Highly Enantioselective Heterogeneous Asymmetric Catalysis. *Journal of the American Chemical Society*, 127(25):8940–8941, 2005.

[85] Jared M. Taylor, Roger K. Mah, Igor L. Moudrakovski, Christopher I. Ratcliffe, Ramanathan Vaidhyanathan, and George K. H. Shimizu. Facile Proton Conduction via Ordered Water Molecules in a Phosphonate Metal−Organic Framework. *Journal of the American Chemical Society*, 132(40):14055–14057, 2010.

[86] Satoshi Horike, Daiki Umeyama, and Susumu Kitagawa. Ion Conductivity and Transport by Porous Coordination Polymers and Metal–Organic Frameworks. *Accounts of Chemical Research*, 46(11):2376–2384, 2013.

[87] Bernard F. Hoskins and Richard Robson. Design and construction of a new class of scaffolding-like materials comprising infinite polymeric frameworks of 3D-linked molecular rods. A reappraisal of the zinc cyanide and cadmium cyanide structures and the synthesis and structure of the diamond-related frameworks $[N(CH_3)_4][Cu^{I}Zn^{II}(CN)_4]$ and Cu^{I}[4,4',4",4"'-tetracyanotetraphenylmethane]$BF_4{\cdot}C_6H_5NO_2$. *Journal of the American Chemical Society*, 112(4):1546–1554, 1990.

[88] Makoto Fujita, Yoon Jung Kwon, Satoru Washizu, and Katsuyuki Ogura. Preparation, Clathration Ability, and Catalysis of a Two-Dimensional Square Network Material Composed of Cadmium(II) and 4,4'-Bipyridine. *Journal of the American Chemical Society*, 116(3):1151–1152, 1994.

[89] Ashlee J. Howarth, Aaron W. Peters, Nicolaas A. Vermeulen, Timothy C. Wang, Joseph T. Hupp, and Omar K. Farha. Best Practices for the Synthesis, Activation, and Characterization of Metal–Organic Frameworks. *Chemistry of Materials*, 29(1):26–39, 2017.

[90] Greig C. Shearer, Sachin Chavan, Silvia Bordiga, Stian Svelle, Unni Olsbye, and Karl Petter Lillerud. Defect Engineering: Tuning the Porosity and Composition of the Metal–Organic Framework UiO-66 via Modulated Synthesis. *Chemistry of Materials*, 28(11):3749–3761, 2016.

[91] Michael J. Katz, Zachary J. Brown, Yamil J. Colon, Paul W. Siu, Karl A. Scheidt, Randall Q. Snurr, Joseph T. Hupp, and Omar K. Farha. A facile

synthesis of UiO-66, UiO-67 and their derivatives. *Chemical Communications*, 49:9449–9451, 2013.

[92] Andreas Schaate, Pascal Roy, Adelheid Godt, Jann Lippke, Florian Waltz, Michael Wiebcke, and Peter Behrens. Modulated Synthesis of Zr-Based Metal–Organic Frameworks: From Nano to Single Crystals. *Chemistry – A European Journal*, 17(24):6643–6651, 2011.

[93] Jasmina Hafizovic Cavka, Søren Jakobsen, Unni Olsbye, Nathalie Guillou, Carlo Lamberti, Silvia Bordiga, and Karl Petter Lillerud. A New Zirconium Inorganic Building Brick Forming Metal Organic Frameworks with Exceptional Stability. *Journal of the American Chemical Society*, 130(42):13850–13851, 2008.

[94] Françesc X. Llabrés i Xamena, Alberto Abad, Avelino Corma, and Hermenegildo Garcia. MOFs as catalysts: Activity, reusability and shape-selectivity of a Pd-containing MOF. *Journal of Catalysis*, 250(2):294 – 298, 2007.

[95] Avelino Corma, Hermenegildo García, and Françesc X. Llabrés i Xamena. Engineering Metal Organic Frameworks for Heterogeneous Catalysis. *Chemical Reviews*, 110(8):4606–4655, 2010.

[96] David J. Tranchemontagne, Jose L. Mendoza-Cortes, Michael O'Keeffe, and Omar M. Yaghi. Secondary building units, nets and bonding in the chemistry of metal-organic frameworks. *Chemical Society Reviews*, 38:1257–1283, 2009.

[97] Danil N. Dybtsev, Alexey L. Nuzhdin, Hyungphil Chun, Konstantin P. Bryliakov, Evgeniy P. Talsi, Vladimir P. Fedin, and Kimoon Kim. A Homochiral Metal–Organic Material with Permanent Porosity, Enantioselective Sorption Properties, and Catalytic Activity. *Angewandte Chemie International Edition*, 45(6):916–920, 2006.

[98] Berta Gomez-Lor, Enrique Gutiérrez-Puebla, Marta Iglesias, María Angeles Monge, Caridad Ruiz-Valero, and Natalia Snejko. $In_2(OH)_3(BDC)_{1.5}$ (BDC = 1,4-Benzendicarboxylate): An In(III) Supramolecular 3D Framework with Catalytic Activity. *Inorganic Chemistry*, 41(9):2429–2432, 2002.

[99] Xin Zhang, Francesc X. Llabrés i Xamena, and Avelino Corma. Gold(III) – metal organic framework bridges the gap between homogeneous and heterogeneous gold catalysts. *Journal of Catalysis*, 265(2):155 – 160, 2009.

[100] Jung Soo Seo, Dongmok Whang, Hyoyoung Lee, Sung Im Jun, Jinho Oh, Young Jin Jeon, and Kimoon Kim. A homochiral metal–organic porous material for enantioselective separation and catalysis. *Nature*, 404(6781):982, 2000.

[101] Shinpei Hasegawa, Satoshi Horike, Ryotaro Matsuda, Shuhei Furukawa, Katsunori Mochizuki, Yoshinori Kinoshita, and Susumu Kitagawa. Three-Dimensional Porous Coordination Polymer Functionalized with Amide Groups Based on Tridentate Ligand: Selective Sorption and Catalysis. *Journal of the American Chemical Society*, 129(9):2607–2614, 2007.

[102] Jerry March. *Advanced organic chemistry: reactions, mechanisms, and structure*. John Wiley & Sons, 1968.

[103] Fransesc Llabres i Xamena and Jorge Gascon. *Metal organic frameworks as heterogeneous catalysts*. Royal Society of Chemistry, 2013.

[104] Takashi Uemura, Kana Kitagawa, Satoshi Horike, Takashi Kawamura, Susumu Kitagawa, Motohiro Mizuno, and Kazunaka Endo. Radical polymerisation of styrene in porous coordination polymers. *Chemical Communications*, (48):5968–5970, 2005.

[105] Annika Herbst and Christoph Janiak. MOF catalysts in biomass upgrading towards value-added fine chemicals. *CrystEngComm*, 19:4092–4117, 2017.

[106] Zhang Yanmei, Degirmenci Volkan, Li Can, and Hensen Emiel J. M. Phosphotungstic Acid Encapsulated in Metal–Organic Framework as Catalysts for Carbohydrate Dehydration to 5-Hydroxymethylfurfural. *ChemSusChem*, 4(1):59–64, 2011.

[107] Akiyama George, Matsuda Ryotaro, Sato Hiroshi, and Kitagawa Susumu. Catalytic Glucose Isomerization by Porous Coordination Polymers with Open Metal Sites. *Chemistry – An Asian Journal*, 9(10):2772–2777, 2014.

[108] Su Ye, Chang Ganggang, Zhang Zhiguo, Xing Huabin, Su Baogen, Yang Qiwei, Ren Qilong, Yang Yiwen, and Bao Zongbi. Catalytic dehydration of glucose to 5-hydroxymethylfurfural with a bifunctional meta-organic framework. *AIChE Journal*, 62(12):4403–4417, 2016.

[109] Annika Herbst and Christoph Janiak. Selective glucose conversion to 5-hydroxymethylfurfural (5-HMF) instead of levulinic acid with MIL-101Cr MOF-derivatives. *New Journal of Chemistry*, 40:7958–7967, 2016.

[110] Mizuho Yabushita, Peng Li, Timur Islamoglu, Hirokazu Kobayashi, Atsushi Fukuoka, Omar K. Farha, and Alexander Katz. Selective Metal–Organic Framework Catalysis of Glucose to 5-Hydroxymethylfurfural Using Phosphate-Modified NU-1000. *Industrial & Engineering Chemistry Research*, 56(25):7141–7148, 2017.

[111] Pravas Deria, Wojciech Bury, Joseph T. Hupp, and Omar K. Farha. Versatile functionalization of the NU-1000 platform by solvent-assisted ligand incorporation. *Chemical Communications*, 50:1965–1968, 2014.

[112] Idan Hod, Pravas Deria, Wojciech Bury, Joseph E Mondloch, Chung-Wei Kung, Monica So, Matthew D Sampson, Aaron W Peters, Cliff P Kubiak, Omar K Farha, et al. A porous proton-relaying metal-organic framework material that accelerates electrochemical hydrogen evolution. *Nature communications*, 6:8304, 2015.

[113] Zhigang Hu, Yongwu Peng, Yongjun Gao, Yuhong Qian, Shaoming Ying, Daqiang Yuan, Satoshi Horike, Naoki Ogiwara, Ravichandar Babarao, Yuxiang Wang, Ning Yan, and Dan Zhao. Direct Synthesis of Hierarchically Porous Metal–Organic Frameworks with High Stability and Strong Brønsted Acidity: The Decisive Role of Hafnium in Efficient and Selective Fructose Dehydration. *Chemistry of Materials*, 28(8):2659–2667, 2016.

[114] Ananda S. Amarasekara, LaToya D. Williams, and Chidinma C. Ebede. Mechanism of the dehydration of D-fructose to 5-hydroxymethylfurfural in dimethyl sulfoxide at 150 °C: an NMR study. *Carbohydrate Research*, 343(18):3021 – 3024, 2008.

[115] Guoli Zi, Zhiying Yan, Yangxia Wang, Yongjuan Chen, Yunlong Guo, Fagui Yuan, Wenyu Gao, Yanmei Wang, and Jiaqiang Wang. Catalytic hydrothermal conversion of carboxymethyl cellulose to value-added chemicals over metal–organic framework MIL-53(Al). *Carbohydrate Polymers*, 115:146 – 151, 2015.

[116] Eric Cockayne. Thermodynamics of the Flexible Metal–Organic Framework Material MIL-53(Cr) From First-Principles. *The Journal of Physical Chemistry C*, 121(8):4312–4317, 2017.

[117] Christian Serre, Franck Millange, Christelle Thouvenot, Marc Noguès, Gérard Marsolier, Daniel Louër, and Gérard Férey. Very Large Breathing Effect in the First Nanoporous Chromium(III)-Based Solids: MIL-53 or $Cr^{III}(OH)\cdot\{O_2C-C_6H_4-CO_2\}\cdot\{HO_2C-C_6H_4-CO_2H\}_x\cdot H_2O_y$. *Journal of the American Chemical Society*, 124(45):13519–13526, 2002.

Co-authorship Statement

The principal author (Jue Gong) contributed to all aspects of the project as the main researcher including: performing experiments, data collection and analysis, designing experiments, summarizing and discussing the data, and writing the manuscript. The corresponding authors (Dr. Michael J. Katz and Dr. Francesca M. Kerton) were principal investigators and provided the initial ideas for experiments conducted. They were responsible for all aspects of the project, including supervision of the principal author (Jue Gong), the design of experiments, examination of the thesis, submission to the journal (RSC Advances), and responding to the questions and comments from the peer reviewers. In addition, Dr. Céline M. Schneider contributes to the acquisition of the solid-state NMR spectra.

Chapter 2

Materials and Methods

2.1 Materials, Reagents and Instrumentation

All reagents were purchased and used without further purification. *N,N*-dimethylacetamide (HPLC grade) and hydrochloric acid (ACS reagent) were purchased from Caledon Laboratories Ltd. *N,N*-dimethylformamide (ACS reagent, $\geq$ 99.8%), methanol (ACS reagent) and dimethyl sulfoxide (ACS reagent, $\geq$ 99.9%) were purchased from ACP Chemicals Inc. The following reagents were purchased from Sigma-Aldrich: Zirconium(IV) chloride ($\geq$ 99.5%), Zirconium(IV) oxychloride octahydrate ($\geq$ 99.5%), terephthalic acid (98%), 2-aminoterephthalic acid (99%), α-D-glucose (96%), trimesic acid (95%), and 1-naphthaldehyde (95%). D-Fructose (99%) was purchased from Alfa Aesar and sucrose (table sugar) was purchased at a supermarket (Sobeys Inc., Canada). Formic acid (98%) was purchased from Fluka. Monosodium 2-sulfoterephthalate (>98%) was purchased from TCI. Dimethyl sulfoxide-*d6* (D, 99.9%) + 0.05% v/v TMS was purchased from Cambridge Isotope Laboratories, Inc.

FT-IR spectra (400-4000 cm^{-1}) were recorded at room temperature on a Bruker Alpha FT-IR Spectrometer with a single-bounce diamond ATR accessory at a res-

olution of 4 cm^{-1} using 36 scans. Powder X-ray diffraction (PXRD) patterns were recorded with a Rigaku Ultima IV diffractometer equipped with a copper sealed-tube operated at 40 kV and 44 mA filtered to 1.54 Å using a graphite monochromator. Simulated powder diffractograms were obtained using the Mercury 3.8 software suite. N_2 gas absorption isotherms were collected on a Micrometrics Tristar II 3020 instrument with the sample maintained at 77 K using $N_{2(l)}$. Before measurements, samples were activated on a Micrometrics Smart VacPrep by first heating at 353 K until a pressure < 5 mmHg was achieved. Subsequently, the sample was heated under the vacuum at 423 K for 10 h. Data was analyzed via the MicroActive Software suite. Solid-state NMR spectra were obtained at 298 K using a Bruker Avance II 600 spectrometer equipped with a SB Bruker 3.2 mm MAS triple-tuned probe operating at 600.33 MHz for ^{1}H and 150.97 MHz for ^{13}C. Chemical shifts were referenced to tetramethylsilane (TMS) using adamantane as an intermediate standard for ^{13}C. The samples were spun at 20 kHz. $^{13}C\{^1H\}$ cross-polarization spectra were collected with a Hartmann-Hahn match at 62.5 kHz and ^{1}H decoupling at 100 kHz. The recycle delay was 3 s and the contact time was 2000 ms. Solution ^{1}H NMR experiments were performed on a Bruker AVANCE III 300.

2.2 Synthesis of MOFs

MOFs were synthesized according to reported literature methods and characterization data were in good agreement with those previously reported.

UiO-66 and UiO-66-NH_2 [1, 2]: $ZrCl_4$ (125 mg, 0.54 mmol) was dissolved in a mixture of concentrated HCl (1 mL) and DMF (5 mL). The mixture was sonicated for 20 min. Then, terephthalic acid (123 mg, 0.75 mmol) or 2-amino-terephthalic acid (134 mg, 0.75 mmol) and another 10 mL of DMF were added. The mixture was

sonicated for a further 20 min. After dissolution, the reaction mixture was then heated at 80 °C overnight in an oven. Upon cooling to room temperature, the resulting solid was filtered and washed with DMF (2×30 mL) and then with methanol (2×30 mL). For UiO-66, the white precipitate was filtered. For UiO-66-NH_2, Chmielewski and co-workers already found that impurity formed in the synthesis of UiO-66-NH_2 due to the formylation of H_2BDC-NH_2 by DMF. [2] Thus, the resulting solid was refluxed in methanol at 60 °C in an oil bath overnight for deformylation, [2] and then collected through vacuum filtration resulting in a pale yellow powder. Finally, both MOFs were dried at 80 °C in a vacuum oven overnight.

UiO-66-SO_3H [3]: A mixture of $ZrOCl_2 \cdot 8H_2O$ (100 mg, 0.31 mmol), BDC-SO_3Na (83 mg, 0.31 mmol) and formic acid (1.17 mL) was dissolved in 3 mL *N,N*-dimethylacetamide (DMA). The mixture was sonicated until full dissolution then was heated at 150 °C for 24 h in an oven. After cooling to room temperature, the white solid was filtered and dried in air. Then, the as- synthesized product was heated at 65 °C in a vacuum oven for 24 h.

MOF-808 [4]: A mixture of H_3BTC (110 mg, 0.50 mmol) and $ZrOCl_2 \cdot 8H_2O$ (160 mg, 0.50 mmol) were dissolved in a solvent mixture of DMF/formic acid (20 mL/20 mL). Then, the mixture was heated at 100 °C for 7 days in an oven. After cooling to room temperature, the resulting solid was filtered with DMF (3×10 mL) and dried at 100 °C for 24 h.

2.3 Catalytic Conversion of Glucose to 5-HMF

Reactions were performed in triplicate, to evaluate reproducibility, by using a Biotage microwave synthesizer. In a typical run, glucose (100 mg) and UiO-66 (20 mg) were weighed in a 2 mL microwave reaction vial. Subsequently, 2 mL DMSO-*d6* was added.

The vial was sealed and heated in the microwave at 160 °C for 30 min. After the reaction finished, the mixture was cooled with pressurized air to 50 °C. Next, the vial was removed from the synthesizer, allowed to cool to ambient temperature, opened, and 15 μL of 1-naphthaldehyde (internal standard) was added into the reaction mixture for quantitative ^{1}H NMR analysis.

2.4 Recycling Experiment and Characterization of Humin

For the recycling test, a reaction was performed on a larger scale, to assess catalytic ability of UiO-66. Glucose (1000 mg), UiO-66 (200 mg), DMSO-*d6* (15 mL) were added to a vial. The mixture was heated in the microwave at 160 °C for 30 min. After the reaction, the mixture was centrifuged and decanted out for quantitative ^{1}H NMR analysis. The solid was washed with 15 mL DMSO three times and separated by vacuum filtration. Then, the solid was dried in a vacuum oven at 80 °C overnight and reused for the next run.

For characterization of humin on the MOF surface, the reaction conditions and the treatment procedure of the used solid catalyst were the same as in the recycling test.

References

[1] Michael J. Katz, Zachary J. Brown, Yamil J. Colon, Paul W. Siu, Karl A. Scheidt, Randall Q. Snurr, Joseph T. Hupp, and Omar K. Farha. A facile synthesis of UiO-66, UiO-67 and their derivatives. *Chemical Communications*, 49:9449–9451, 2013.

[2] Krzysztof M. Zwolinski, Piotr Nowak, and Michał J. Chmielewski. Towards multifunctional MOFs - transforming a side reaction into a post-synthetic protection/deprotection method. *Chemical Communications*, 51:10030–10033, 2015.

[3] Shyam Biswas, Jian Zhang, Zhibao Li, Ying-Ya Liu, Maciej Grzywa, Lixian Sun, Dirk Volkmer, and Pascal Van Der Voort. Enhanced selectivity of CO_2 over CH_4 in sulphonate-, carboxylate- and iodo-functionalized UiO-66 frameworks. *Dalton Transactions*, 42:4730–4737, 2013.

[4] Hiroyasu Furukawa, Felipe Gándara, Yue-Biao Zhang, Juncong Jiang, Wendy L. Queen, Matthew R. Hudson, and Omar M. Yaghi. Water Adsorption in Porous Metal–Organic Frameworks and Related Materials. *Journal of the American Chemical Society*, 136(11):4369–4381, 2014.

Chapter 3

Results and Discussion

3.1 Dehydration of Glucose to 5-HMF using UiO-66 and its analogues

UiO-66-X (X=H, NH_2, SO_3H) were synthesized using a solvothermal method. [1–3] UiO-66-X is build up from $Zr_6O_4(OH)_4$ octahedral nodes and 2-X-1,4-benzenedicarboxylate (BDC-X) organic linkers (Figure 3.1). UiO-66 possesses extraordinary stability due to the formation of Zr-O bonds between the metallic cluster and carboxylate organic ligands. [4] More specifically, such unprecedented stability is attributed to the combination of strong Zr-O bonds and the ability of the inner Zr_6-cluster to rearrange reversibly upon removing or adding the μ_3-OH without changes in the connecting carboxylates. [5] Therefore, UiO-66 and its derivatives are potential candidates for conversion of glucose to 5-HMF due to the unprecedented chemical stability, exceptionally high surface areas as well as the presence of Lewis acidic zirconium metal nodes. Moreover, several authors have already reported synthesis of functionalized MOFs and their use in catalysis. [6,7] Thus, we hypothesized that the Brønsted acidic SO_3H-functionalized UiO-66 might facilitate dehydration of glucose, thereby enhanc-

ing the yield of 5-HMF via bifunctional acid catalysis (Lewis-acidic isomerization from glucose to fructose and then Brønsted acidic transformation to 5-HMF). [8, 9] In the case of UiO-66-NH_2, we assumed that the presence of the amino group could aid the proton transfer in glucose conversion. Consequently, UiO-66 and its analogues are considered as our primary catalyst choice in the conversion of glucose to 5-HMF.

Before performing reactions using UiO-66-X, a series of characterization methods (FT-IR, PXRD and N_2 adsorption) are conducted. Our results are compared with those published in previous literature and any differences should be discussed.

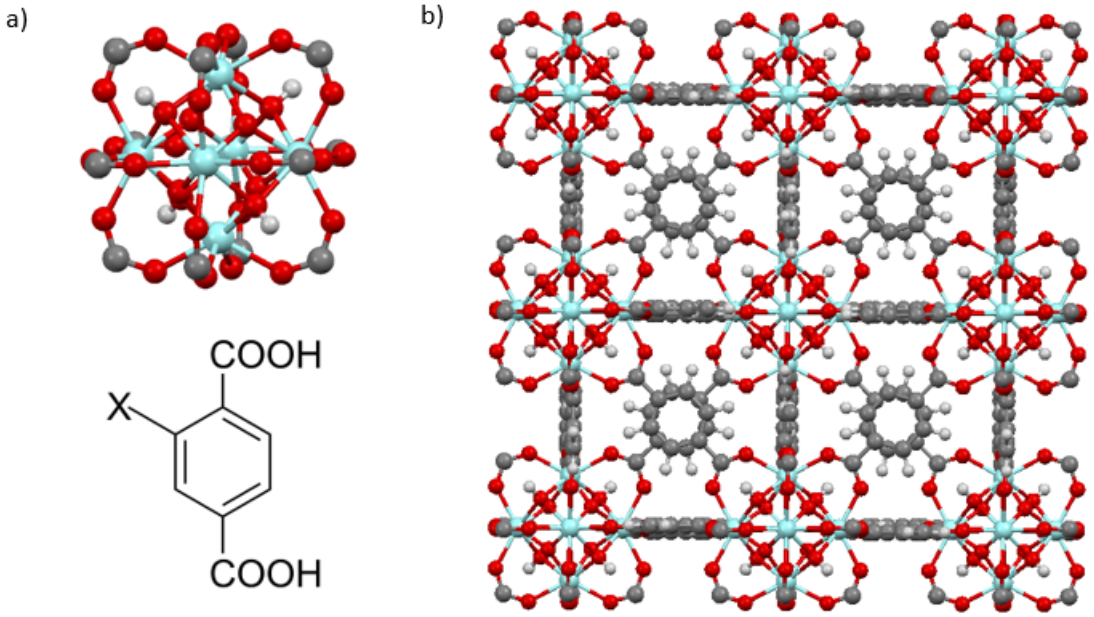

Figure 3.1: (a) Schematic illustration of $Zr_6O_4(OH)_4$ octahedra containing twelve carboxylate groups coordinated to the zirconium cations (top) and 2-X-1,4-benzenedicarboxylate (BDC-X) organic struts, X=H, NH_2 or SO_3H (bottom). (b) The structural representation of cubic unit cell of UiO-66. Zr, blue; O, red; C, gray; H, white.

Figure 3.2 demonstrates that the FT-IR spectrum of UiO-66 and its analogues are similar. The spectra shows two strong absorption bands in the region of 1560-1600 cm^{-1} and 1380-1415 cm^{-1} that are attributed to carboxylate asymmetric and

symmetric stretching vibrations. [3, 10] The intense absorption band observed in the region of 1653-1665 cm^{-1} is a result of the C=O stretch of DMF inside the pores of the MOF. [5, 11] Another medium absorption band in the region of 1495-1507 cm^{-1} is attributed to C-C ring vibration within the linkers. [11]

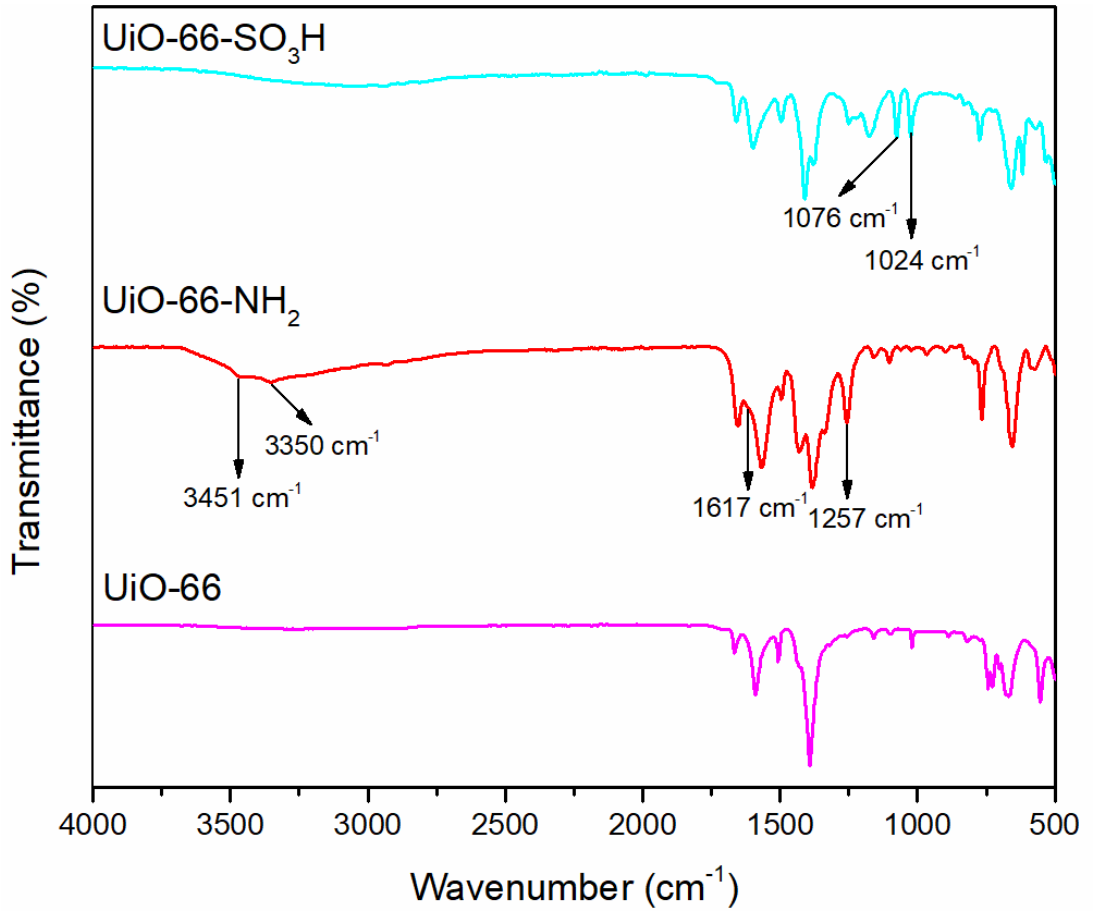

Figure 3.2: FT-IR spectra of UiO-66 and its analogues.

In the high frequency region of UiO-66-NH_2, two absorption bands are presented at 3350 cm^{-1} and 3451 cm^{-1} due to asymmetric and symmetric stretches of the primary amino group (-NH_2). This indicates the successful synthesis of amino-functionalized UiO-66. [4, 12] In the low frequency region, a weak N-H bending vibration at 1617 cm^{-1} and a strong C-N stretching absorption at 1257 cm^{-1} also confirm the presence of the amino group. [4] For UiO-66-SO_3H, the O=S=O asymmetric and symmetric

stretching bands are seen at 1076 cm^{-1} and 1024 cm^{-1} respectively. [3]

Through a PXRD study, UiO-66 and its derivatives were shown to be crystalline with their corresponding diffraction patterns matching that of simulated UiO-66 (Figure 3.3). However, a missing peak is observed at 2θ of 12° in the XRD pattern of simulated UiO-66 since the simulated pattern of UiO-66 is calculated based on the single-crystal X-ray diffraction.

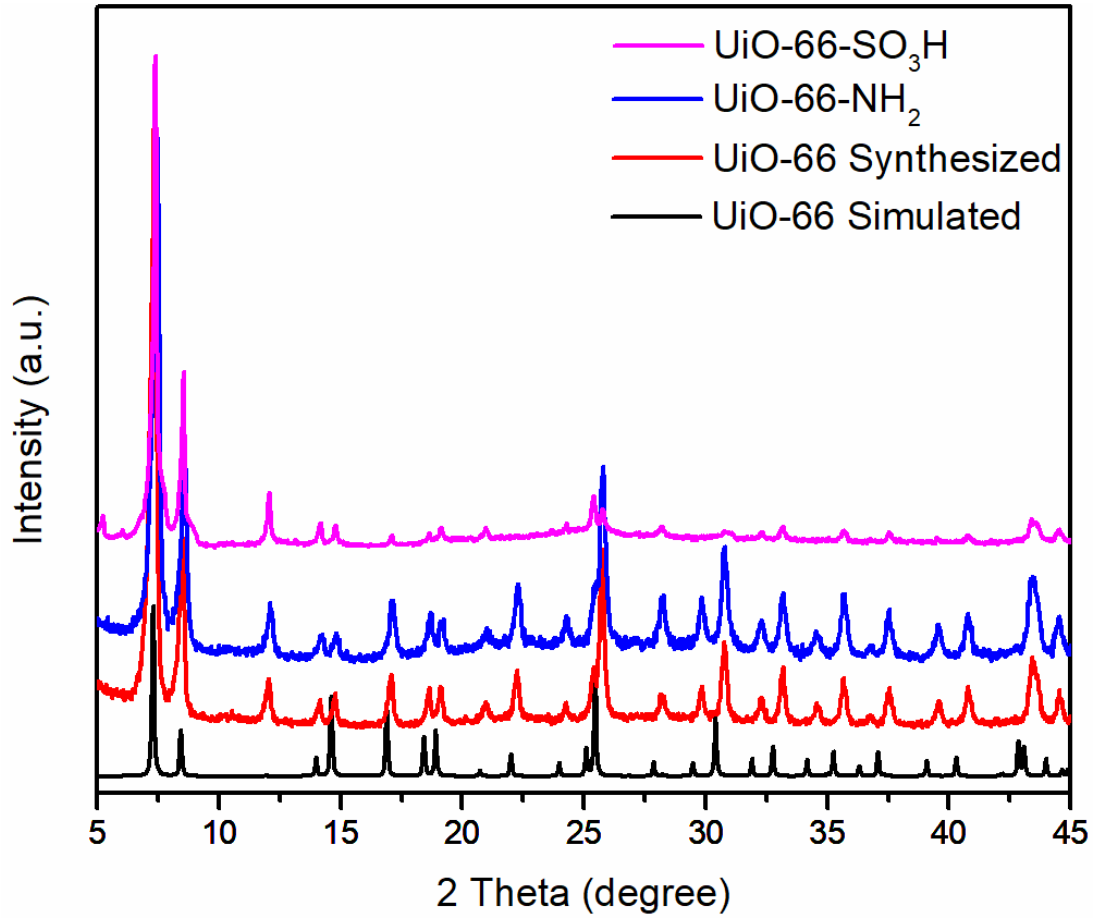

Figure 3.3: PXRD patterns of experimental UiO-66-X (X=H, NH_2, and SO_3H) and simulated UiO-66.

Dehydration of glucose was investigated using UiO-66-X as the catalyst and DMSO as the solvent in a microwave oven at 160 °C for 20 min. In a control reaction, only 2% of 5-HMF was formed in the absence of a MOF catalyst (Table 3.1 & Figure 3.4).

In contrast, another control reaction using fructose instead of glucose produced a very high yield (61%) of 5-HMF under the same reaction conditions. This demonstrated that DMSO itself is an efficient catalyst in the catalytic conversion of fructose to 5-HMF, as reported by Amarasekara *et al.* in 2008. [13] Thus, the focus of our catalytic study is on glucose as the substrate.

Table 3.1: Yields for glucose conversion to 5-HMF.

Entry	Catalyst	5-HMF yield (%)
1	Control	2.4 ± 0.5
2	UiO-66	20 ± 0.1
3	UiO-66-NH_2	16 ± 0.06
4	UiO-66-SO_3H	4.7 ± 0.5

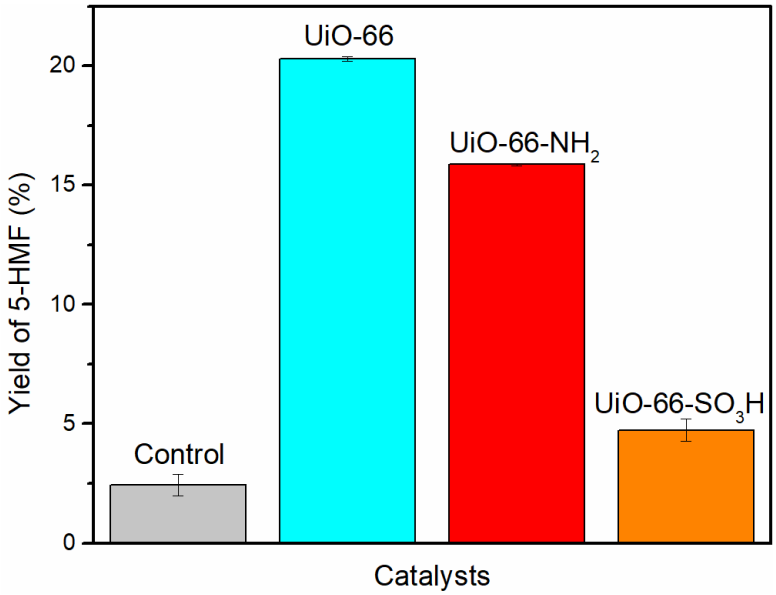

Figure 3.4: Yield of 5-HMF in the catalytic conversion of glucose to 5-HMF. Conditions: Microwave, 100 mg glucose, 10 mg UiO-66-X (X=H, NH_2, SO_3H), 2 mL DMSO-*d6*, 160 °C, 20 min.

Our initial study attempted to determine the most active of the three MOFs (UiO-66, UiO-66-NH_2 and UiO-66-SO_3H) in the dehydration of glucose. The initial microwave reaction was performed with a 10 mg catalyst loading for 100 mg glucose. Under same reaction conditions, the highest yield of 5-HMF (20%) was achieved using

UiO-66 (Table 3.1 & Figure 3.4), while the NH_2- and SO_3H-functionalized UiO-66 gave lower yields. The yield of 5-HMF obtained using UiO-66-NH_2 was 16%, which was 4% lower than obtained using UiO-66. Somewhat surprisingly, only 5% of 5-HMF was obtained using UiO-66-SO_3H. This observation is contrary to our initial hypotheses. Therefore, we speculate that the surface area of the UiO-66-X materials plays the critical role in determining reactivity, since the presence of -NH_2 and -SO_3H groups resulted in lower surface areas (1045 m^2g^{-1} and 515 m^2g^{-1} respectively as compared with 1650 m^2g^{-1} for UiO-66) and hence, lower yields (Figure 3.5). The similar surface areas of UiO-66-X (X=H, NH_2, SO_3H) were also observed by others previously. [1,3]

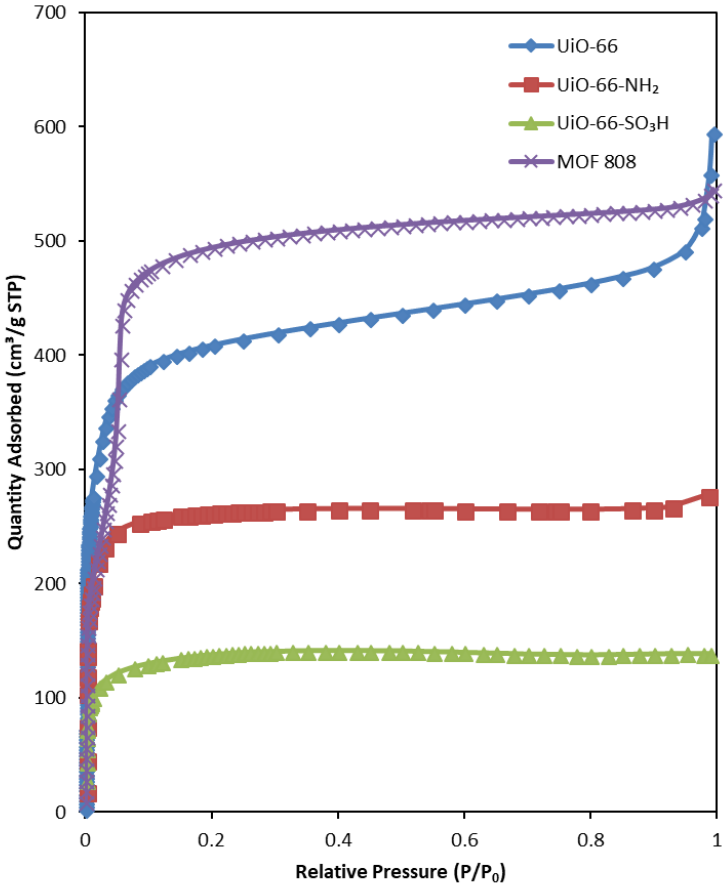

Figure 3.5: Nitrogen gas adsorption isotherms at 77 K of UiO-66-X and MOF 808.

3.2 Optimization of Reaction Conditions

As the initial screening revealed that the highest yield (20%) of 5-HMF was obtained using UiO-66, we then attempted to optimize reaction conditions by varying different reaction parameters (reaction time, catalyst loading, and temperature) to improve the yield of 5-HMF. The results for catalytic conversion of glucose to 5-HMF with different catalyst loadings at various temperatures and reaction times are presented in Table 3.2.

Table 3.2: Optimization of reaction time, catalyst loading and temperature of UiO-66 for the conversion of glucose to 5-HMF[a,b]

	Reaction Conditions			
Entry	UiO-66 loading (mg)	Temp (°C)	Time (min)	Yield of 5-HMF (%)
1	10	160	20	20
2	10	160	30	21
3	10	160	40	16
4	10	160	50	15
5	20	150	30	9
6	20	160	30	28
7	20	160	30	37[c]
8	20	170	30	26
9	20	180	30	26
10	20	190	30	16
11	30	160	30	25

[a.] Unless stated otherwise, the conversion of glucose to 5-HMF was conducted in the presence of 100 mg glucose and 2 mL DMSO-*d6*.
[b.] For quantitative ^{1}H NMR analysis, 15 μL 1-naphthaldehyde was used as the internal standard.
[c.] Reaction was performed in 2 mL solvent mixture of DMSO-*d6*/water (2.5% v/v water).

3.2.1 Effect of reaction time on yield of 5-HMF.

Various reaction times from 20 to 50 min were tested. According to the results shown in Table 3.2 and Figure 3.6, we conclude that the yield of 5-HMF increases initially, reaches the maximum at 30 min, and then decreases after 30 min. We assume this observation is owing to the decomposition of 5-HMF after 30 min; this trend has been observed by others as well. [14, 15] The highest yield (21%) of 5-HMF was obtained using 10 mg UiO-66 at 160 °C for 30 min. After 30 min, the yield of

5-HMF dropped to 16% (40 min) and 15% (50 min) respectively. As shown in Figure 3.7, there are three pathways for the decomposition of 5-HMF (the rehydration of 5-HMF to levulinic acid and formic acid, self-polymerization of 5-HMF itself, and cross-polymerization between 5-HMF and glucose). [14, 16, 17] In our study since less than 4% formic acid was formed and no levulinic acid was observed by ^{1}H NMR in the reaction mixtures, the rehydration of 5-HMF was suppressed in the presence of DMSO. A similar observation in the presence of [BMIM][Cl] was found by Qi *et al.* in 2009. [14] Thus, the reduction of 5-HMF yield after an optimum time has passed is more liekly due to cross-polymerization between 5-HMF and remaining glucose to form humin. A more detailed discussion of humin formation will be presented in Section 3.4.

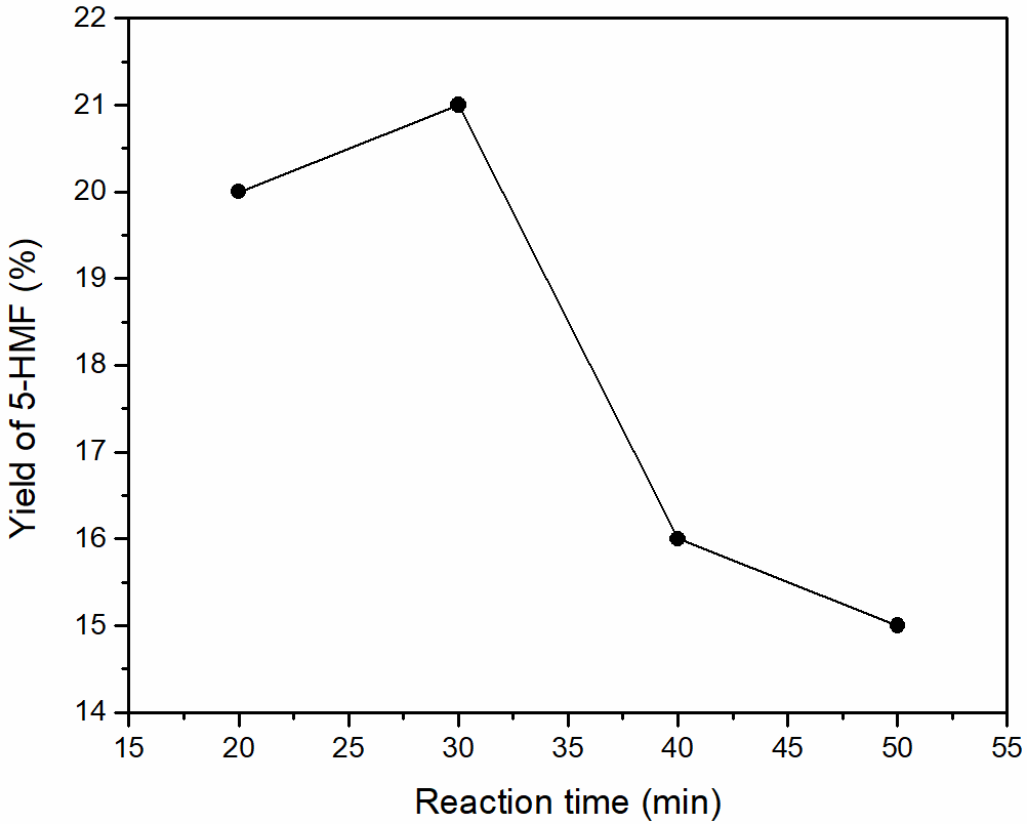

Figure 3.6: Effect of reaction time on yield of 5-HMF. Reaction conditions: Microwave, 100 mg glucose, 10 mg UiO-66, 2 mL DMSO-*d6*, 160 °C.

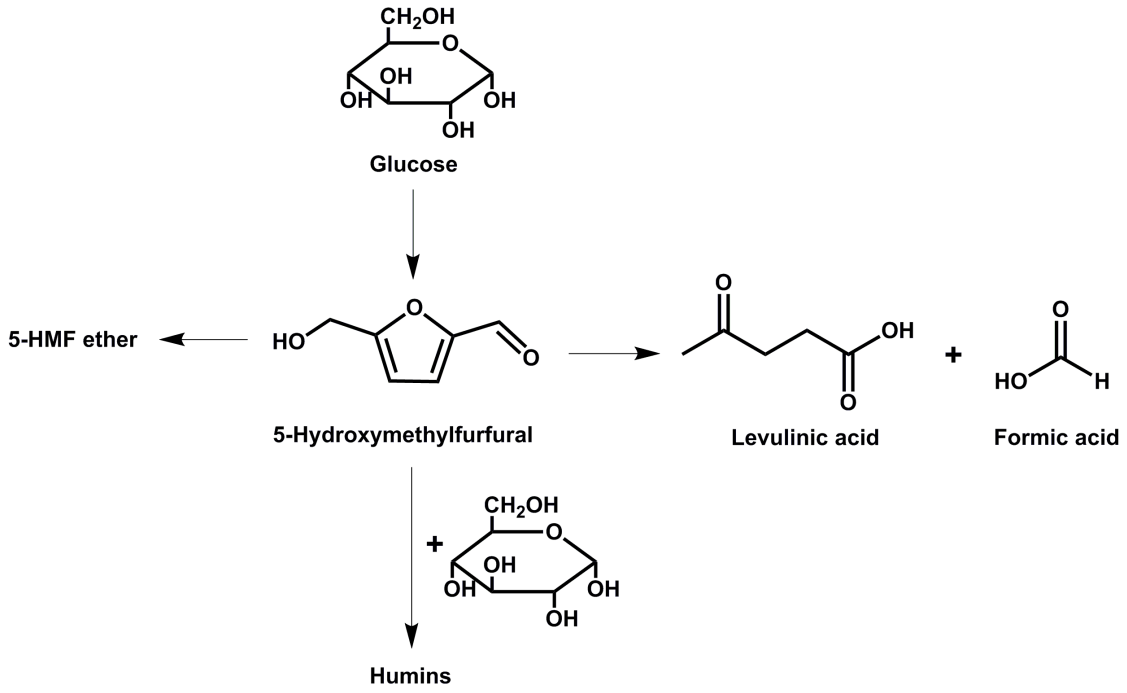

Figure 3.7: Pathways for decomposition of 5-HMF during glucose conversion.

3.2.2 Effect of catalyst loading on yield of 5-HMF

To investigate the effect of UiO-66 loadings on the yield of 5-HMF, the microwave reaction was performed in the presence of 100 mg glucose at 160 °C for 30 min using 10, 20 or 30 mg of UiO-66. In a control reaction without UiO-66, the yield was only 3% but increased to 21% and 28% with 10 or 20 mg UiO-66 respectively (Table 3.2, entry 2 and 6). However, the yield of 5-HMF decreased slightly to 25% when 30 mg UiO-66 was used (Table 3.2, entry 11). Dehydration of glucose is accelerated in an acidic environment. [18] Therefore, more UiO-66 presented in the reaction system, and consequently a greater number of Lewis acidic Zr(IV) sites can facilitate the dehydration of glucose and enhance the yield of 5-HMF. However, in our optimization study, the observation is contrary to our assumption. We found that the yield of 5-HMF drops at higher catalyst loading most likely due to side reactions including humin formation between glucose and 5-HMF.

3.2.3 Effect of temperature on yield of 5-HMF

High temperatures are essential in the conversion of glucose to 5-HMF. [14,15,18] Therefore, to evaluate the temperature effect on the 5-HMF yield, we performed reactions at various temperature from 150 °C to 190 °C.

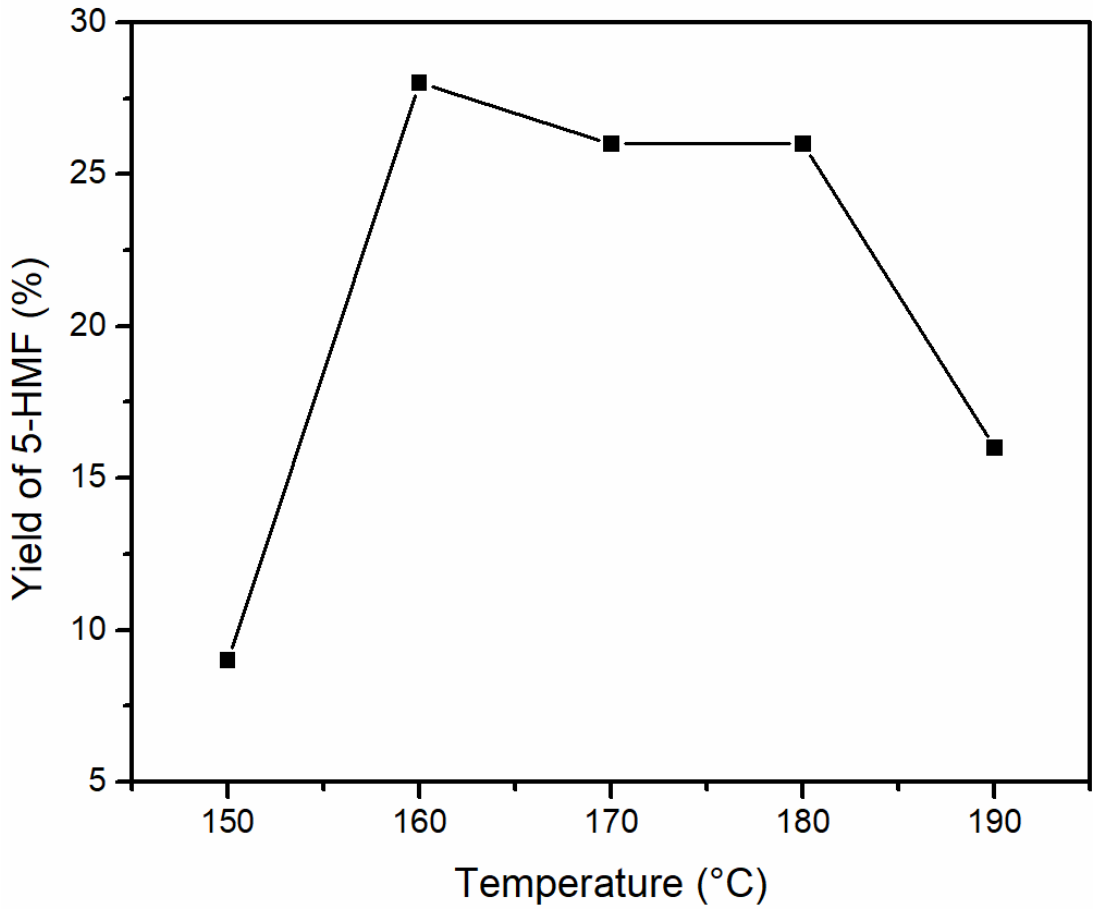

Figure 3.8: Effect of temperature on yield of 5-HMF. Conditions: Microwave, 100 mg glucose, 10 mg UiO-66, 2 mL DMSO-*d6*, 30 min.

As shown in Table 3.2 and Figure 3.8, the yield of 5-HMF increased significantly from 150 °C to 160 °C, reached 28% yield at 160 °C, but decreased when higher temperature is applied. The yield of 5-HMF drops to 16% at 190 °C. This trend is attributed to decomposition of 5-HMF above 160 °C. A small contribution to this decreased yield is observed from the rehydration of 5-HMF at higher temperature

via ^{1}H NMR. Through ^{1}H NMR, around 8% formic acid was formed above 160 °C but no levulinic acid was found. Thus, the major cause of such low yields is the polymerization of 5-HMF to form insoluble humin by-products.

It has been reported that very high yield of 5-HMF is achieved in the solvent mixture of THF/water (v:v 39:1) in the catalytic conversion of glucose and cellulose to 5-HMF. [19, 20] However, increasing water contents or only water as the solvent lowers the yield of 5-HMF since too much water added into the reaction mixture or pure water as single solvent could lower the concentration of glucose. [19,20] Therefore, in our reaction, the solvent mixture of DMSO-*d6*/water (v:v 39:1) was investigated. The maximum yield (37%) of 5-HMF was attained (Table 3.2, entry 7), which was nearly 10% higher than the yield (28%) with pure DMSO-*d6*, under the same reaction conditions. Our results are consistent with those reported by others, which proves that just a small amount of water can facilitate the conversion of glucose to 5-HMF. [19,20]

It is essential to compare our results with those already performed using different MOFs. In Table 3.3, we summarize the yield of 5-HMF in the catalytic conversion of glucose to 5-HMF using three different MOFs (UiO-66, MIL-101 and NU-1000). Unlike UiO-66-SO_3H catalyst studied herein, the SO_3H-functionalized MIL catalyst afforded a good yield (29%) of 5-HMF but only 2% yield of 5-HMF was obtained using bare, unsulfontated MIL-101. [19] The possible explanation is that MIL-SO_3H possesses more Brønsted acidic sites and maintains a fairly high surface area of 1333 m^2g^{-1} as compared to bare MIL-101. [19] Very recently, Katz, Farha *et al.* demonstrated that the phosphate-modified NU-1000 provides much higher yield of 5-HMF, relative to unmodified NU-1000. [21] Furthermore, they also observed that the yield of 5-HMF increased to 20% using a solvent mixture of 2-PrOH/water (v:v 9:1) with PO_4/NU(half) catalyst. [21] They also demonstrated that a lower glucose loading could reduce humin formation in the conversion of glucose, which significantly en-

hanced the yield of 5-HMF (Table 3.3, entry 8). [21]

3.3 Recycling Test

In order to assess the stability of UiO-66 during glucoe conversion to 5-HMF, a catalyst recycling experiment was conducted and the results are shown in Figure 3.9.

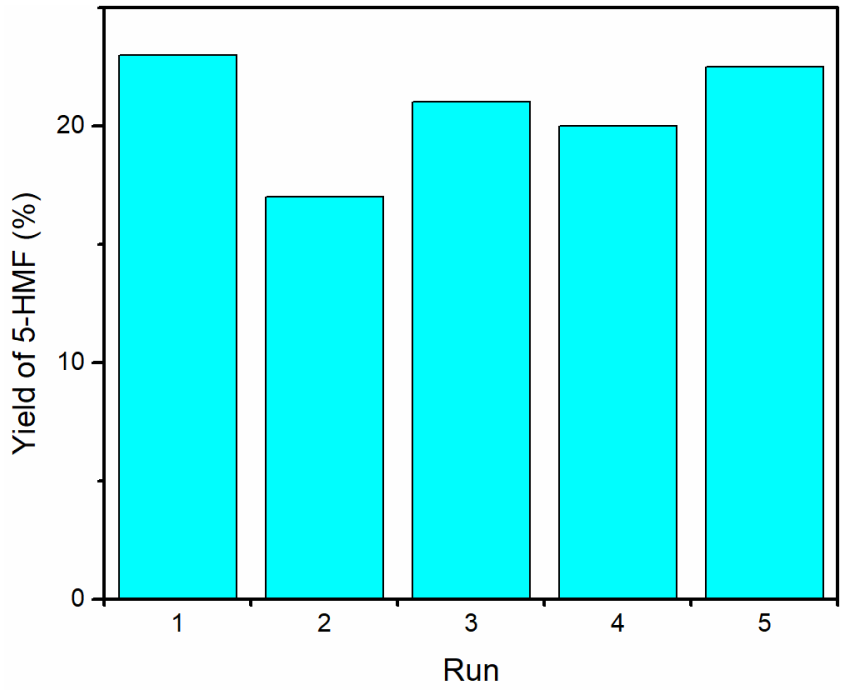

Figure 3.9: Recycling experiment of UiO-66. Conditions: Microwave, 1000 mg glucose, 200 mg UiO-66, 15 mL DMSO-*d6*, 160 °C, 30 min.

As shown in Figure 3.9, UiO-66 could be re-used up to 5 times with a small loss in the yield of 5-HMF. We assumed that small differences of 5-HMF yields could be attributed to the experimental error during the recycling test. We observed that the color of the solid catalyst changed from white to dark brown after the reaction (Figure 3.10). Moreover, we observed that humin could not be removed from the solid catalyst by washing with DMSO since the colour of the solid catalyst doesn't change after washing. Janiak and Herbst performed regeneration experiments by washing

Table 3.3: Comparison of glucose conversion to 5-HMF using UiO-66 and literature reports using three different MOFs

Entry [ref.]	Glucose loading (mmol)	Reaction Conditions				5-HMF yield (%)
		Solvent	Catalyst	Temp (°C)	Time	
1	0.56	DMSO-*d6*	UiO-66	160	30 min	28
2	0.56	39:1(v/v) DMSO-*d6*/water	UiO-66	160	30 min	37
3 [19]	1.24	39:1(v/v) THF/water	MIL-101	130	24 h	2.0
4 [19]	1.24	39:1(v/v) THF/water	MIL-SO_3H	130	24 h	29
5 [21]	0.10	water	NU-1000	140	5 h	2.3
6 [21]	0.10	water	PO_4/NU(half)[a]	140	5 h	15
7 [21]	0.10	9:1(v/v) 2-PrOH/water	PO_4/NU(half)[a]	140	5 h	20
8 [21]	0.10×10^{-2}	9:1(v/v) 2-PrOH/water	PO_4/NU(half)[a]	140	5 h	64

[a.] PO_4/NU(half) refers to half of the OH groups of NU-1000 were treated with phosphate groups of phosphoric acid.

the solid catalyst after reaction with several solvents such as methanol, THF, H_2O and H_2SO_4 at room temperature and at 80 °C but no significant improvement of the surface area was found. [19]

We speculate that the existence of humin on the UiO-66 surface or inside the pores of UiO-66 would cause a decrease in the surface area, which could affect the yield of 5-HMF. Therefore, we examined the surface area of UiO-66 before and after reaction, in which the latter material we refer to as UiO-66-humin from herein. From N_2 adsorption isotherms, the BET surface area for UiO-66 and UiO-66-humin was found to decrease signficantly from 1650 m^2g^{-1} to 598 m^2g^{-1} respectively (Figure 3.11).

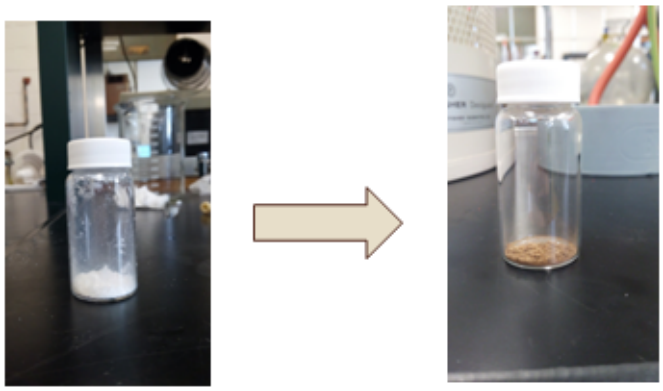

Figure 3.10: Colour on the right is due to the humin formation.

3.4 Characterization of Humin on MOF Surface

Humin is an unavoidable byproduct in the catalytic conversion of biomass. [22] The structure of humin has not yet been well-studied so far. Sumerskii proposed that humin is composed of 60% furan rings and 20% ether or acetal aliphatic linkers. [23] Moreover, the mechanism of humin formation is still not fully understood. In the

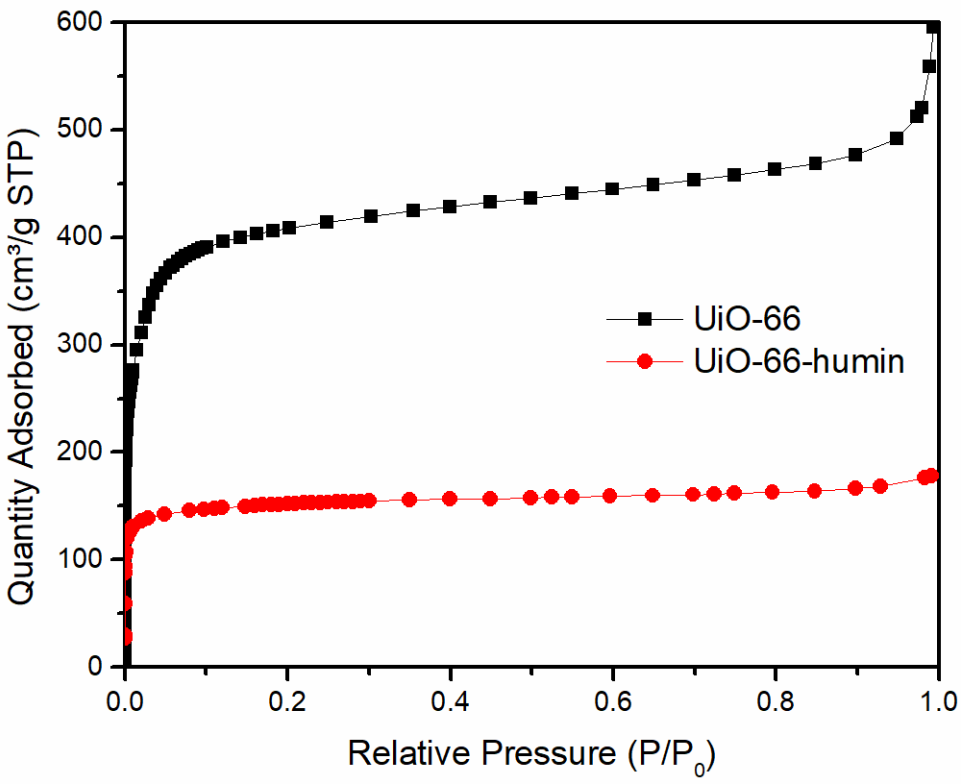

Figure 3.11: Nitrogen gas adsorption isotherms at 77 K of UiO-66 and UiO-66-humin.

acidic dehydration of glucose to 5-HMF using MOFs, the formation of humin and the color change of solid catalysts have been observed after reaction by our group and others. [19, 21, 24] However, to the best of our knowledge, although several papers have reported the formation of humin on MOF surfaces indirectly, e.g., through N_2 adsorption isotherms, the systematic characterization of humin on the surface of a MOF has not been reported until recently. Therefore, for my research project, one of main focuses was to investigate the existence of humin on UiO-66 using different characterization techniques.

Due to the formation of humin after reaction, we observed that the colour of UiO-66 changed from white to dark brown (Figure 3.10). We speculate that the humin formation on the surface significantly inhibits the yield of 5-HMF obtained. First, we examined the surface area of UiO-66 and UiO-66-humin. As the results shown in Fig-

ure 3.11, the adsorption ability of UiO-66-humin apparently decreased after reaction. Fhe BET surface area of UiO-66-humin dropped to 598 m^2g^{-1}, which was considerably lower than that of UiO-66 before the reaction (1653 m^2g^{-1}). These differences in the N_2 adsorption isotherms indicate that the existence of humin could inevitably affect the catalytic efficiency of UiO-66 in the conversion of glucose, revealing that the reaction undergoes via a heterogeneous mechanism wherein surface area is a critical parameter for catalytic activity. The similar observation was also reported by Janiak and Herbst in 2016. [19] They found that the surface area of MIL-SO_3H was reduced from 1333 m^2g^{-1} to 443 m^2g^{-1} after reaction in a solvent mixture of THF/water (v:v=39:1). [19]

PXRD patterns of simulated UiO-66, synthesized UiO-66 and UiO-66-humin display no significant changes in peak positions (Figure 3.12). However, the crystallinity of UiO-66-humin is diminished with regard to original UiO-66 because the two main peaks at 2θ of 7.4° and 8.5° have become broader, and likely less intense, after reaction. We assume that the occurrence of an additional small peak at a 2θ of 6.2° in UiO-66-humin represents 'forbidden' reflections for the topological space group due to diffuse scattering by the humin. [25]

Through FT-IR spectroscopy, we find that the bands in the spectrum of UiO-66-humin are much broader than those in the spectrum of UiO-66 (Figure 3.13). In the spectrum of UiO-66-humin, a broad peak around 3352 cm^{-1} is due to C-O stretch from alcohols. [23,26] A weak absorption band at 2919 cm^{-1} can be attributed to aliphatic C-H stretches. [23, 26] Moreover, some differences between the spectra of these two materials might be attributed to the presence of furan rings, such as the C=C stretching absorption at 1583 cm^{-1} and the C-O stretching absorption at 1017 cm^{-1}, [26] with the latter band showing significantly more intensity than a weak absorption in the same region of UiO-66. Additionally, below 1000 cm^{-1} in

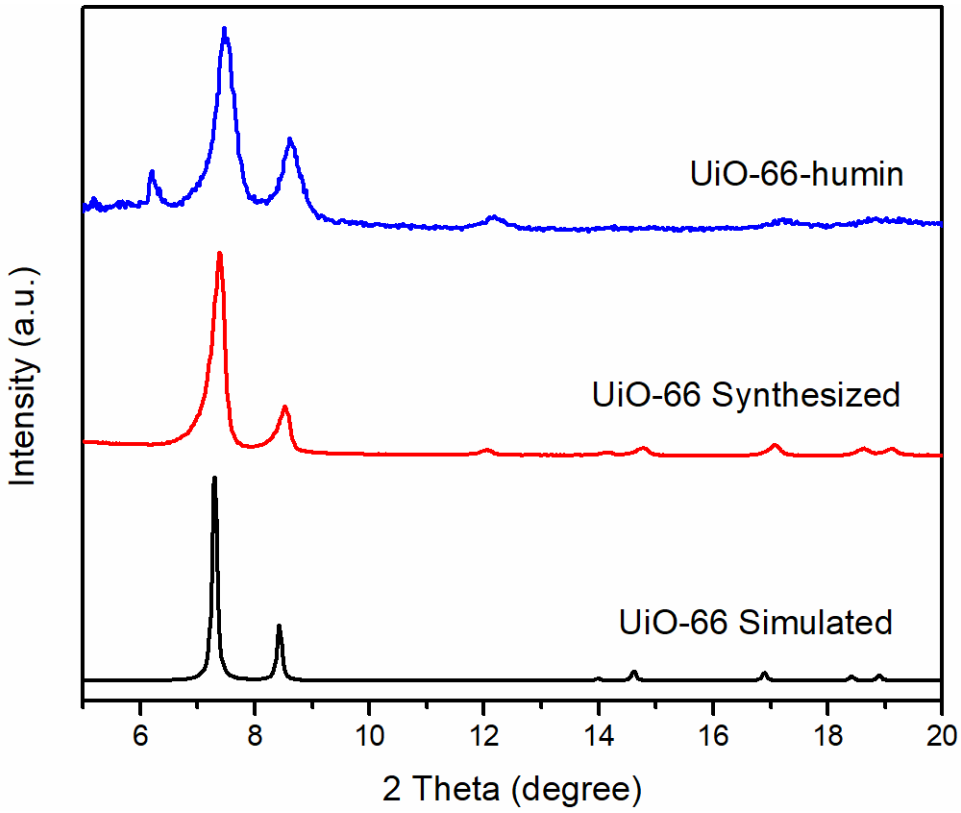

Figure 3.12: PXRD patterns of UiO-66 simulated (black), UiO-66 synthesized (red), and UiO-66-humin (blue).

the fingerprint region, peaks at 952 cm^{-1} and 746 cm^{-1} might be the results of the presence of substituted furan rings. [27]

To further investigation the formation of humin on UiO-66, ^{13}C solid-state NMR spectroscopy was applied to distinguish the UiO-66 samples before and after reaction (Figure 3.14). The ^{13}C solid-state NMR spectrum of UiO-66 consists of three characteristic peaks at chemical shifts of 128.9, 137.1 and 170.8 ppm. Based on the NMR study by Devautour-Vinot and Martineau *et al.*, [28] the peak at 128.9 ppm is attributed to the -CH group of the aromatic rings. The peak at 137.1 ppm is ascribed to the quaternary aromatic carbon atoms. The peak at 170.8 ppm is assigned to carbon atoms from the carboxylate groups. [28] The presence of a low-intensity peak at 167.6 ppm is from the C=O group of DMF solvent molecules left in the pores of

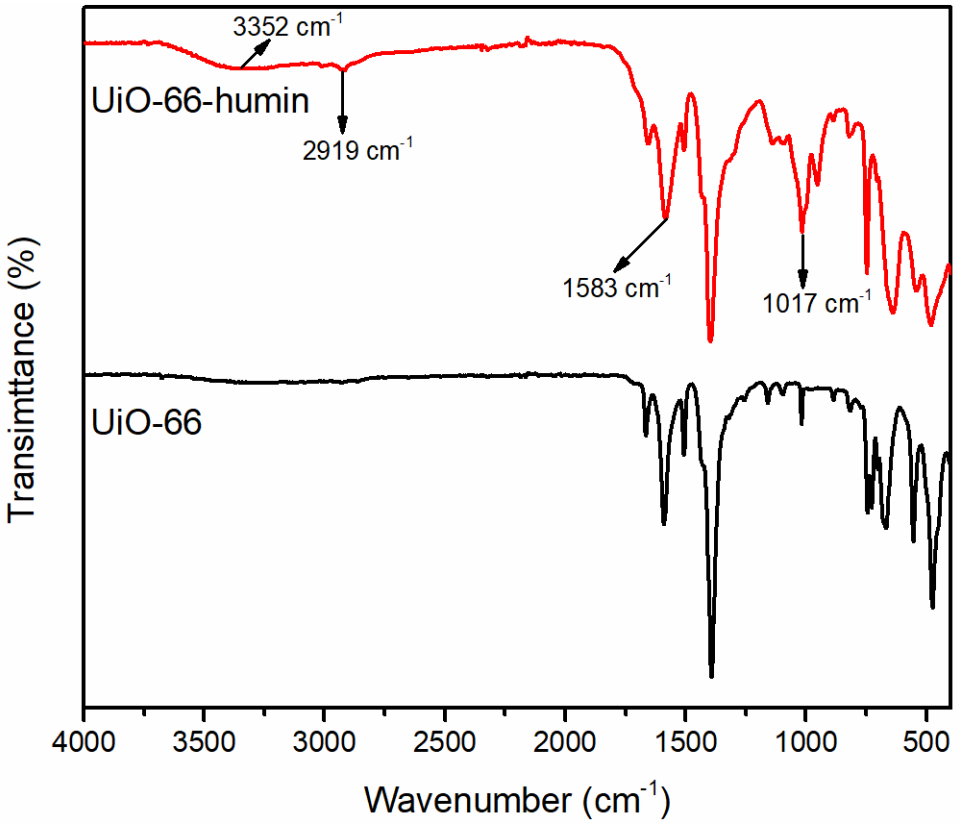

Figure 3.13: FT-IR spectra of UiO-66 and UiO-66-humin.

UiO-66. Comparing the ^{13}C solid-state NMR spectrum of UiO-66-humin with the spectrum of UiO-66, significant peak broadening is observed in the spectrum, which indicates that a less crystalline solid material is formed after reaction, corroborating the PXRD data (Figure 3.12).

Moreover, the appearance of an intense peak located around 39 ppm represents the presence of tertiary and/or quaternary aliphatic carbons. [29] In addition, a broad characteristic signal between 60 and 90 ppm is due to many different C-O groups from alcohol or ether functionalities in the humin structure. [27, 29] These two mid-to-high field peaks, which are not observed in the spectrum of UiO-66, strongly suggest the formation of humin on UiO-66 in the conversion of glucose to 5-HMF. It should be noted that the peaks at around 130, 138 and 170 ppm are broader and although these are

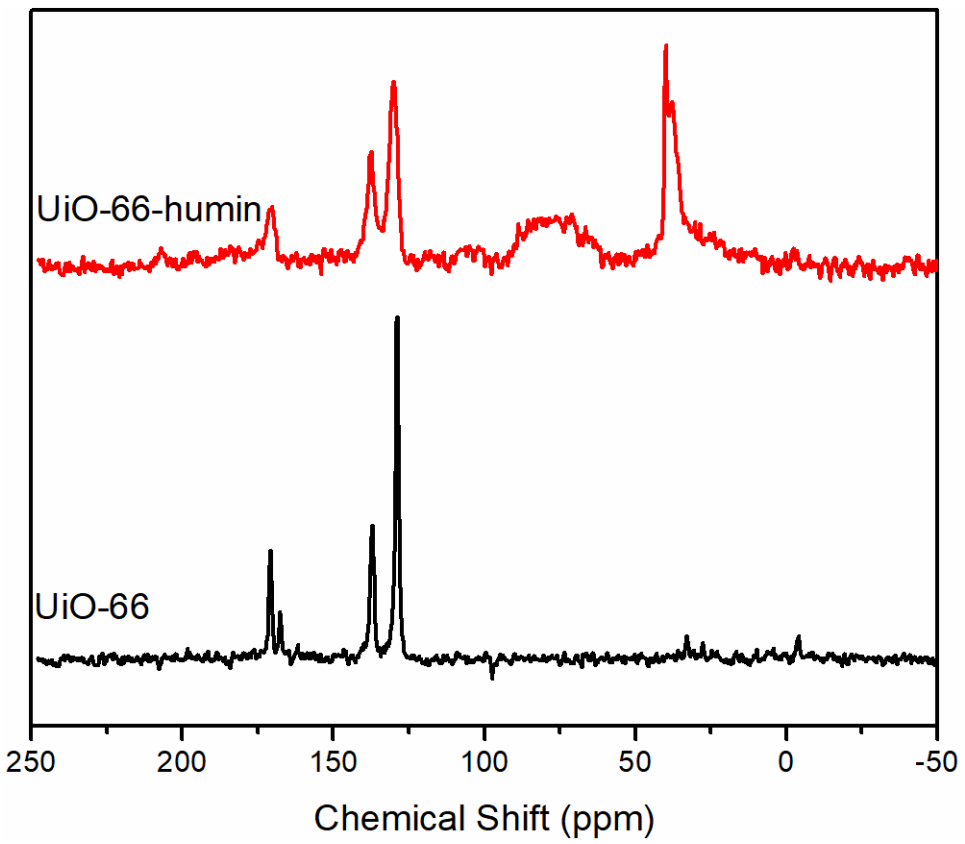

Figure 3.14: ^{13}C solid-state NMR spectrums of UiO-66 (bottom) and UiO-66-humin (top).

located at similar chemical shifts to the carbon atoms of the 1,4-benzenedicarboxylate (BDC) linker in the spectrum of UiO-66, they might be coincident with substituted carbon atoms of furan rings and carbon atoms from carboxyl or ester groups in the humin. [29]

We also conducted three comparative reactions for investigating the effect of humin formation on the yield of 5-HMF and to assess the inhibitory effect of humin by blocking access to pores within the MOF. Initially, a microwave reaction was performed with 20 mg UiO-66 at 160 °C for 30 min, affording 28% yield of 5-HMF. After that, we set up two different routes. Either 20 mg of fresh UiO-66 or 100 mg of glucose was added into the reaction system and the vial was heated under the same optimal

conditions for 30 min. We found that the yield of 5-HMF increased from 28% to 35% when 20 mg of fresh UiO-66 was added, which indicates that some unreacted glucose and intermediate dehydration products are still left in the initial reaction mixture but unable to react to form 5-HMF once UiO-66-humin has formed. In contrast, the overall yield of 5-HMF dropped from 28% to 23% when an additional 100 mg glucose was added after the initial 30 min reaction. We assume the additional 100 mg glucose could cross-polymerize with the 5-HMF to form insoluble humins and the used UiO-66 with a diminishing surface area may not catalyze the dehydration of the additional glucose effectively. In our third study, the reaction was performed by using 40 mg UiO-66 for 2×30 min at 160 °C and the yield of 5-HMF was only 26%. This shows that the existence of humin reduces the amount of 5-HMF that can form and that this is most likely due tot the humin formation blocking the pores of the MOF.

3.5 Dehydration of Glucose to 5-HMF using MOF 808

Based on our study of glucose conversion to 5-HMF using UiO-66-X (X=H, NH_2, SO_3H) solid catalysts, we find that surface area is the critical parameter in the dehydration of glucose. Another zirconium-containing MOF, MOF 808, has emerged as a potential candidate for gas adsorption [30] and catalysis [31] because of its unique features. Compared with 12-connected or 8-connected MOFs, [32] MOF 808 possesses lower connectivity (6-connected) and hence greater pore access to more reactant or adsorbent molecules. Therefore, due to its larger surface area and greater pore size, we hypothesized that 6-connected zirconium-containing MOF, MOF 808, could improve the yield of 5-HMF in the glucose conversion as compared with UiO-66-X.

As with UiO-66-X, MOF 808 [32] is built up from octahedral $[Zr_6O_4(OH)_4]^{12+}$

cationic nodes and trimesic acid (H_3BTC) organic linkers (Figure 3.15). The secondary building units are connected to six BTC linkers. Also, six formate ligands cap the node and account for the charge balance. [32] Compared with UiO-66-X, MOF 808 provides a wider pore size with the internal pore diameter of 18.4 Å vs. 6 Å for UiO-66. [5, 32]

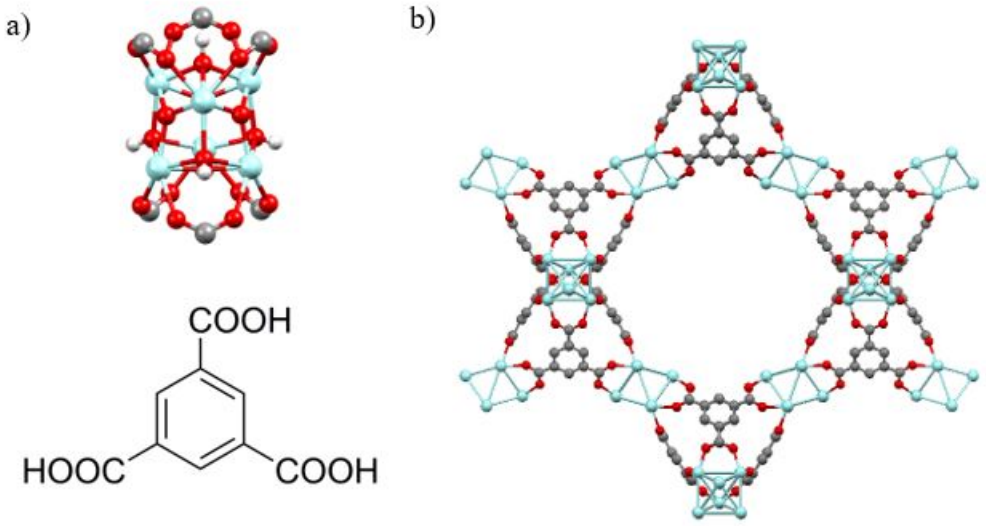

Figure 3.15: (a) Illustration of $Zr_6O_4(OH)_4$ secondary building units (top) and trimesic acid (H_3BTC) organic linkers (bottom). (b) Structural representation of MOF 808. Zr, blue; O, red; C, gray; H, white. μ_3-O and H atoms are omitted for clarity.

A sample of synthesized MOF 808 was examined by FT-IR (Figure 3.16), PXRD (Figure 3.17) and N_2 adsorption (Figure 3.5) before use. The FT-IR spectra of synthesized MOF 808 is almost same as those reported by others. [33, 34] Two intense absorption bands locating at 1606 cm^{-1} and 1378 cm^{-1} are attributed to carboxylate asymmetric and symmetric stretching. The PXRD pattern of synthesized MOF 808 is almost the same as the pattern of simulated MOF 808. Moreover, the BET surface area of MOF 808 was up to 1970 m^2g^{-1}.

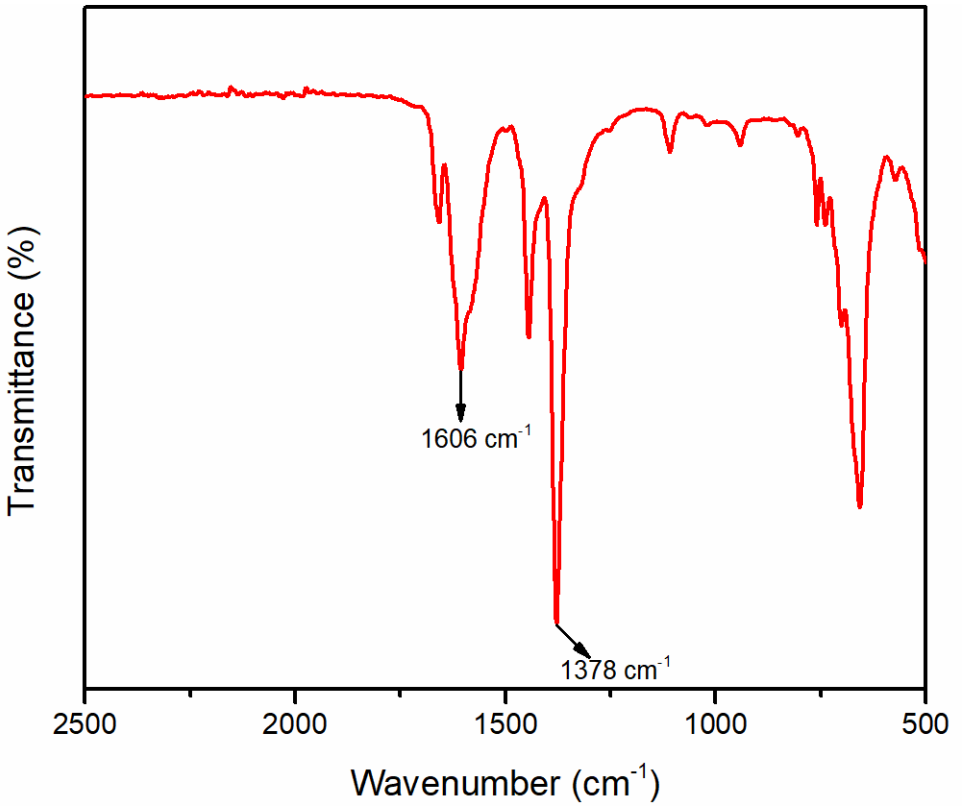

Figure 3.16: FT-IR spectra of MOF 808.

The catalytic dehydration reaction was performed at 160 °C for 30 min. According to the yield study, MOF 808 gave the highest yield (31%) of 5-HMF of the four MOF catalysts studied herein under our standardized conditions. Furthermore, the yield obtained by MOF 808 is 10% higher than that produced by UiO-66 (21%) at the same reaction conditions. We think that the greater yield afforded by MOF 808 is owing to its larger pore size and higher surface area compared with UiO-66. Moreover, it may also be attributed to lower coordination numbers of the zirconium centres, which means they can interact more readily with substrates in the catalytic cycle. However, the yield of 5-HMF was only 28% in the presence of the solvent mixture of DMSO-*d6*/water (v:v=39:1), which is slightly lower than the yield achieved using pure DMSO-*d6*. Also, this observation is inconsistent with that we observed using UiO-66 in the presence of the solvent mixture of DMSO-*d6*/water (v:v=39:1). We hypothesize

that the aggregation of water molecules in the pores of MOF 808 could block the channels of MOF 808 and thereby decrease the 5-HMF yield. [32] Unfortunately, the color of MOF 808 changed to dark brown after reaction, which implied the humin formation. Used MOF 808 after reaction are denoted as MOF 808-humin.

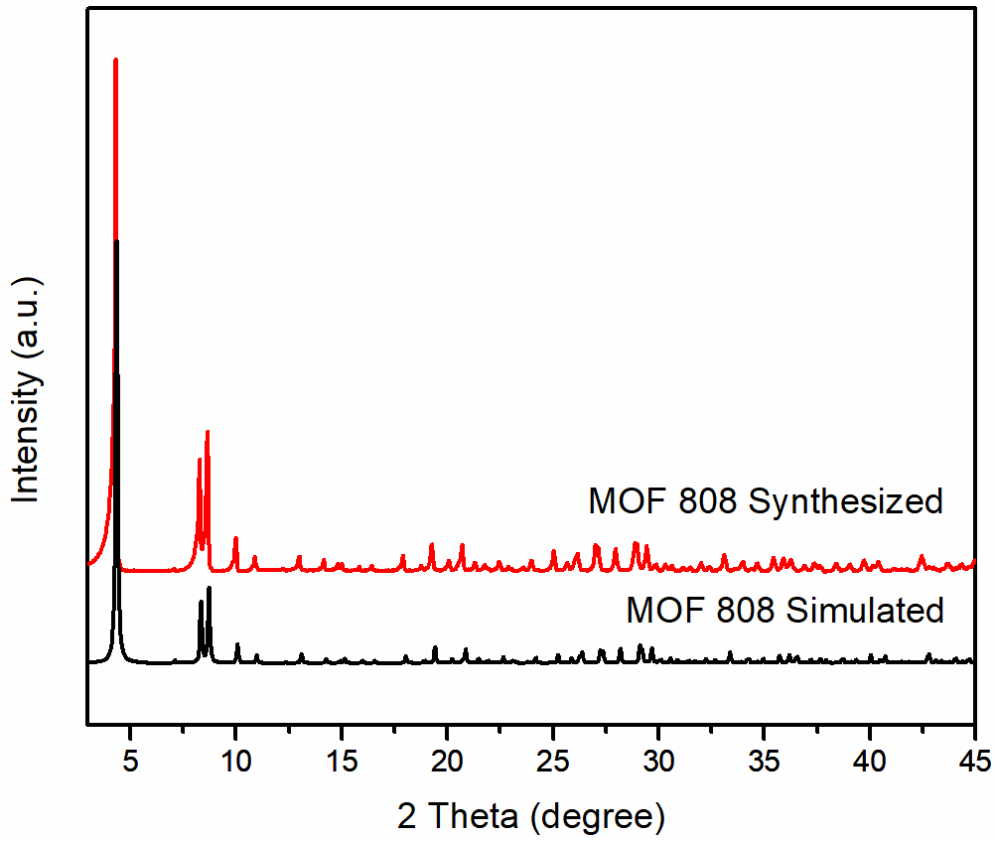

Figure 3.17: PXRD patterns of simulated and synthesized MOF 808.

We compare spectra of MOF 808 and MOF 808-humin by using FT-IR spectroscopy (Figure 3.18). In the spectrum of MOF 808-humin, a broad absorption band around 3340 cm^{-1} is attributed to C-O stretch from alcohols. [23,26] Comparing these two spectrums, some other differences between these two also means the existence of furan rings, such as the C=C stretching absorption at 1577 cm^{-1} and the C-O stretching absorption at 1023 cm^{-1}. [26] In addition, below 1000 cm^{-1} in the fingerprint region, peaks at 990 cm^{-1} and 758 cm^{-1} are the results of the formation of substi-

tuted furan rings. [27] We compared FT-IR spectrums between UiO-66-humin and MOF 808-humin and found that some similarities between these two indicate that the structure of humin consists of furan rings and some alcohol functional groups (Figure 3.19).

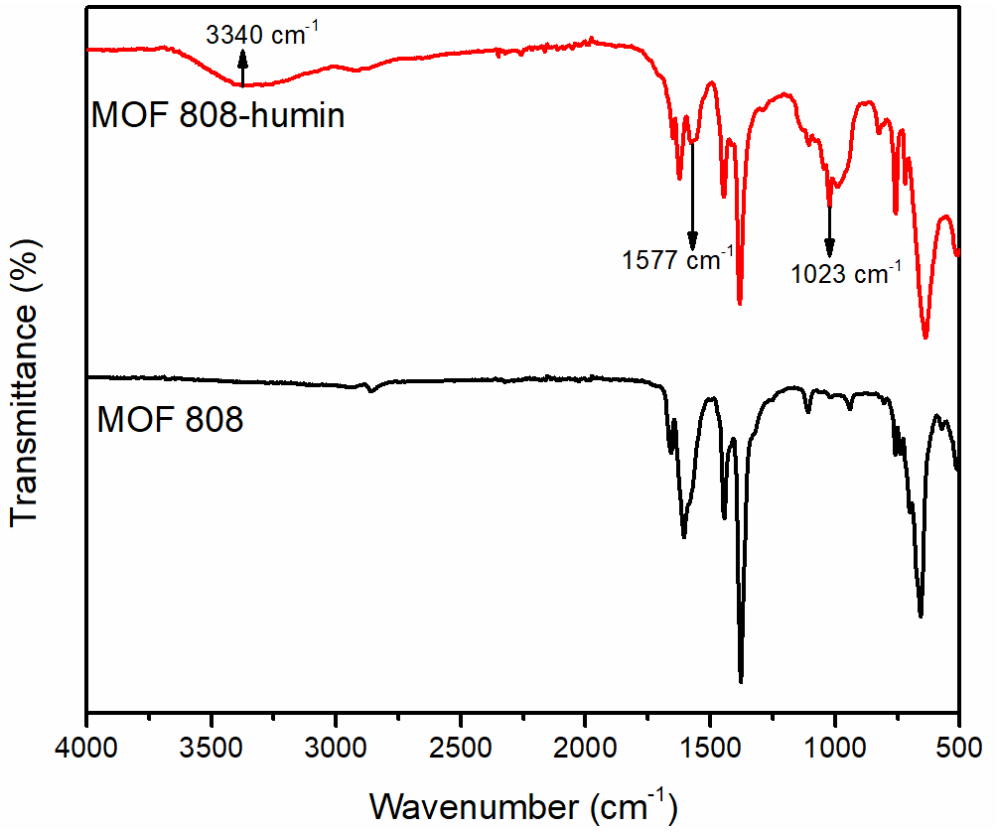

Figure 3.18: FT-IR spectra of MOF 808 and MOF 808-humin.

Besides, we attempted the conversion of sucrose to 5-HMF with MOF 808. The reaction conditions were the same as those applied in the conversion of glucose to 5-HMF with MOF 808. The 5-HMF yield is 46%, which is 8% higher than that produced in sucrose conversion without MOF catalyst in a control reaction wherein DMSO could catalyze the conversion. However, we also found that there was no significant difference in the 5-HMF yield using UiO-66 (44%) and MOF 808 (46%) in the sucrose conversion to 5-HMF.

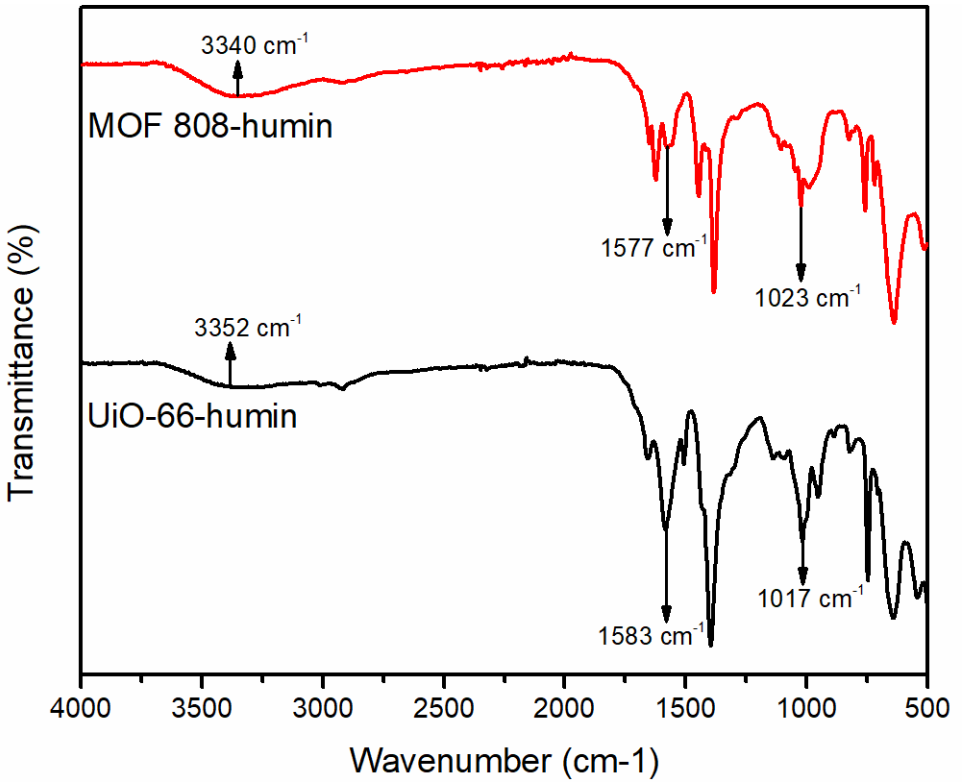

Figure 3.19: FT-IR spectra of UiO-66-humin and MOF 808-humin.

References

[1] Michael J. Katz, Zachary J. Brown, Yamil J. Colon, Paul W. Siu, Karl A. Scheidt, Randall Q. Snurr, Joseph T. Hupp, and Omar K. Farha. A facile synthesis of UiO-66, UiO-67 and their derivatives. *Chemical Communications*, 49:9449–9451, 2013.

[2] Krzysztof M. Zwolinski, Piotr Nowak, and Michał J. Chmielewski. Towards multifunctional MOFs - transforming a side reaction into a post-synthetic protection/deprotection method. *Chemical Communications*, 51:10030–10033, 2015.

[3] Shyam Biswas, Jian Zhang, Zhibao Li, Ying-Ya Liu, Maciej Grzywa, Lixian Sun, Dirk Volkmer, and Pascal Van Der Voort. Enhanced selectivity of CO_2 over CH_4

in sulphonate-, carboxylate- and iodo-functionalized UiO-66 frameworks. *Dalton Transactions*, 42:4730–4737, 2013.

[4] Mathivathani Kandiah, Merete Hellner Nilsen, Sandro Usseglio, Søren Jakobsen, Unni Olsbye, Mats Tilset, Cherif Larabi, Elsje Alessandra Quadrelli, Francesca Bonino, and Karl Petter Lillerud. Synthesis and Stability of Tagged UiO-66 Zr-MOFs. *Chemistry of Materials*, 22(24):6632–6640, 2010.

[5] Jasmina Hafizovic Cavka, Søren Jakobsen, Unni Olsbye, Nathalie Guillou, Carlo Lamberti, Silvia Bordiga, and Karl Petter Lillerud. A New Zirconium Inorganic Building Brick Forming Metal Organic Frameworks with Exceptional Stability. *Journal of the American Chemical Society*, 130(42):13850–13851, 2008.

[6] Marco Ranocchiari and Jeroen Anton van Bokhoven. Catalysis by metal-organic frameworks: fundamentals and opportunities. *Physical Chemistry Chemical Physics*, 13:6388–6396, 2011.

[7] Michael J Ingleson, Jorge Perez Barrio, Jean-Baptiste Guilbaud, Yaroslav Z Khimyak, and Matthew J Rosseinsky. Framework functionalisation triggers metal complex binding. *Chemical Communications*, (23):2680–2682, 2008.

[8] Vinit Choudhary, Samir H. Mushrif, Christopher Ho, Andrzej Anderko, Vladimiros Nikolakis, Nebojsa S. Marinkovic, Anatoly I. Frenkel, Stanley I. Sandler, and Dionisios G. Vlachos. Insights into the Interplay of Lewis and Brønsted Acid Catalysts in Glucose and Fructose Conversion to 5-(Hydroxymethyl)furfural and Levulinic Acid in Aqueous Media. *Journal of the American Chemical Society*, 135(10):3997–4006, 2013.

[9] Jinqiang Tang, Xiawei Guo, Liangfang Zhu, and Changwei Hu. Mechanistic Study of Glucose-to-Fructose Isomerization in Water Catalyzed by $[Al(OH)_2(aq)]^+$. *ACS Catalysis*, 5(9):5097–5103, 2015.

[10] Shyam Biswas, Tim Ahnfeldt, and Norbert Stock. New Functionalized Flexible Al-MIL-53-X (X = -Cl, -Br, -CH3, -NO2, -(OH)2) Solids: Syntheses, Characterization, Sorption, and Breathing Behavior. *Inorganic Chemistry*, 50(19):9518–9526, 2011.

[11] Loredana Valenzano, Bartolomeo Civalleri, Sachin Chavan, Silvia Bordiga, Merete H. Nilsen, Søren Jakobsen, Karl Petter Lillerud, and Carlo Lamberti. Disclosing the Complex Structure of UiO-66 Metal Organic Framework: A Synergic Combination of Experiment and Theory. *Chemistry of Materials*, 23(7):1700–1718, 2011.

[12] Hussein Rasool Abid, Jin Shang, Ha-Ming Ang, and Shaobin Wang. Amino-functionalized Zr-MOF nanoparticles for adsorption of CO_2 and CH_4. *International Journal of Smart and Nano Materials*, 4(1):72–82, 2013.

[13] Ananda S. Amarasekara, LaToya D. Williams, and Chidinma C. Ebede. Mechanism of the dehydration of D-fructose to 5-hydroxymethylfurfural in dimethyl sulfoxide at 150 °C: an NMR study. *Carbohydrate Research*, 343(18):3021 – 3024, 2008.

[14] Xinhua Qi, Masaru Watanabe, Taku M. Aida, and Richard L. Smith, Jr. Efficient process for conversion of fructose to 5-hydroxymethylfurfural with ionic liquids. *Green Chemistry*, 11:1327–1331, 2009.

[15] Feng Guo, Zhen Fang, and Tie-Jun Zhou. Conversion of fructose and glucose into 5-hydroxymethylfurfural with lignin-derived carbonaceous catalyst under

microwave irradiation in dimethyl sulfoxide–ionic liquid mixtures. *Bioresource Technology*, 112:313 – 318, 2012.

[16] Feridoun Salak Asghari and Hiroyuki Yoshida. Kinetics of the Decomposition of Fructose Catalyzed by Hydrochloric Acid in Subcritical Water: Formation of 5-Hydroxymethylfurfural, Levulinic, and Formic Acids. *Industrial & Engineering Chemistry Research*, 46(23):7703–7710, 2007.

[17] Jarosław Lewkowski. Synthesis, chemistry and applications of 5-hydroxymethylfurfural and its derivatives. *Arkivoc*, 2001:17–54, 2001.

[18] Andreia A. Rosatella, Svilen P. Simeonov, Raquel F. M. Frade, and Carlos A. M. Afonso. 5-Hydroxymethylfurfural (HMF) as a building block platform: Biological properties, synthesis and synthetic applications. *Green Chemistry*, 13:754–793, 2011.

[19] Annika Herbst and Christoph Janiak. Selective glucose conversion to 5-hydroxymethylfurfural (5-HMF) instead of levulinic acid with MIL-101Cr MOF-derivatives. *New Journal of Chemistry*, 40:7958–7967, 2016.

[20] Weingarten Ronen, Rodriguez-Beuerman Alexandra, Cao Fei, Luterbacher Jeremy S., Alonso David Martin, Dumesic James A., and Huber George W. Selective Conversion of Cellulose to Hydroxymethylfurfural in Polar Aprotic Solvents. *ChemCatChem*, 6(8):2229–2234, 2014.

[21] Mizuho Yabushita, Peng Li, Timur Islamoglu, Hirokazu Kobayashi, Atsushi Fukuoka, Omar K. Farha, and Alexander Katz. Selective Metal–Organic Framework Catalysis of Glucose to 5-Hydroxymethylfurfural Using Phosphate-Modified NU-1000. *Industrial & Engineering Chemistry Research*, 56(25):7141–7148, 2017.

[22] George Tsilomelekis, Michael J. Orella, Zhexi Lin, Ziwei Cheng, Weiqing Zheng, Vladimiros Nikolakis, and Dionisios G. Vlachos. Molecular structure, morphology and growth mechanisms and rates of 5-hydroxymethyl furfural (HMF) derived humins. *Green Chemistry*, 18:1983–1993, 2016.

[23] Ivan V. Sumerskii, Stepan M. Krutov, and Mikhail Ya. Zarubin. Humin-like substances formed under the conditions of industrial hydrolysis of wood. *Russian Journal of Applied Chemistry*, 83(2):320–327, 2010.

[24] Jinzhu Chen, Kegui Li, Limin Chen, Ruliang Liu, Xing Huang, and Daiqi Ye. Conversion of fructose into 5-hydroxymethylfurfural catalyzed by recyclable sulfonic acid-functionalized metal-organic frameworks. *Green Chemistry*, 16:2490–2499, 2014.

[25] Matthew J Cliffe, Wei Wan, Xiaodong Zou, Philip A Chater, Annette K Kleppe, Matthew G Tucker, Heribert Wilhelm, Nicholas P Funnell, François-Xavier Coudert, and Andrew L Goodwin. Correlated defect nanoregions in a metal–organic framework. *Nature communications*, 5:4176, 2014.

[26] Ilona van Zandvoort, Ernst R. H. van Eck, Peter de Peinder, Hero J. Heeres, Pieter C. A. Bruijnincx, and Bert M. Weckhuysen. Full, Reactive Solubilization of Humin Byproducts by Alkaline Treatment and Characterization of the Alkali-Treated Humins Formed. *ACS Sustainable Chemistry & Engineering*, 3(3):533–543, 2015.

[27] Sushil K. R. Patil, Jacob Heltzel, and Carl R. F. Lund. Comparison of Structural Features of Humins Formed Catalytically from Glucose, Fructose, and 5-Hydroxymethylfurfuraldehyde. *Energy & Fuels*, 26(8):5281–5293, 2012.

[28] Sabine Devautour-Vinot, Guillaume Maurin, Christian Serre, Patricia Horcajada, Denise Paula da Cunha, Vincent Guillerm, Elisângela de Souza Costa, Francis Taulelle, and Charlotte Martineau. Structure and Dynamics of the Functionalized MOF Type UiO-66(Zr): NMR and Dielectric Relaxation Spectroscopies Coupled with DFT Calculations. *Chemistry of Materials*, 24(11):2168–2177, 2012.

[29] Ilona van Zandvoort, Eline J. Koers, Markus Weingarth, Pieter C. A. Bruijnincx, Marc Baldus, and Bert M. Weckhuysen. Structural characterization of ^{13}C-enriched humins and alkali-treated ^{13}C humins by 2D solid-state NMR. *Green Chemistry*, 17:4383–4392, 2015.

[30] Katherine Healey, Weibin Liang, Peter D. Southon, Tamara L. Church, and Deanna M. D'Alessandro. Photoresponsive spiropyran-functionalised MOF-808: postsynthetic incorporation and light dependent gas adsorption properties. *Journal of Materials Chemistry A*, 4:10816–10819, 2016.

[31] Pengfei Ji, Joseph B. Solomon, Zekai Lin, Alison Johnson, Richard F. Jordan, and Wenbin Lin. Transformation of Metal–Organic Framework Secondary Building Units into Hexanuclear Zr-Alkyl Catalysts for Ethylene Polymerization. *Journal of the American Chemical Society*, 139(33):11325–11328, 2017.

[32] Hiroyasu Furukawa, Felipe Gándara, Yue-Biao Zhang, Juncong Jiang, Wendy L. Queen, Matthew R. Hudson, and Omar M. Yaghi. Water Adsorption in Porous Metal–Organic Frameworks and Related Materials. *Journal of the American Chemical Society*, 136(11):4369–4381, 2014.

[33] Yaguang Peng, Hongliang Huang, Dahuan Liu, and Chongli Zhong. Radioactive Barium Ion Trap Based on Metal–Organic Framework for Efficient and Irre-

versible Removal of Barium from Nuclear Wastewater. *ACS Applied Materials & Interfaces*, 8(13):8527–8535, 2016.

[34] Juncong Jiang, Felipe Gándara, Yue-Biao Zhang, Kyungsu Na, Omar M. Yaghi, and Walter G. Klemperer. Superacidity in Sulfated Metal–Organic Framework-808. *Journal of the American Chemical Society*, 136(37):12844–12847, 2014.

Chapter 4

Conclusions

In the initial study of glucose conversion to 5-HMF using UiO-66-X (X=H, NH_2 and SO_3H), UiO-66 afforded the highest yield of 5-HMF among these three. Reaction time, temperature and catalyst loading were varied to optimize the reaction conditions. For examination of the catalytic efficiency of UiO-66, we conducted recycling tests and found that the efficiency of UiO-66 dropped slightly after five runs since humin, an unavoidable byproduct, was formed inside the pores or on the surface of UiO-66. Moreover, the color of UiO-66 changed from white to dark brown after three runs. Therefore, we compared UiO-66 and UiO-66-humin using different analytical techniques, which demonstrate the formation of humin on UiO-66. Another zirconium-containing MOF, MOF 808, which gave a higher surface area and more accessible zirconium centrs, provided a significantly higher yield of 5-HMF as compared to UiO-66-X (X=H, NH_2 and SO_3H) under the same reaction conditions. These data prove that surface area is a critical parameter for efficient catalytic dehydration of glucose to yield 5-HMF using different MOF catalysts. Additionally, functionality cannot enhance the catalysis since the presence of -NH_2 and -SO_3H causes the diminishing surface area.

For my future work, it would be better to obtain further evidence in the characterization of the humin through comparing analytical data with standards for humin and humic acids. In addition, catalyst recycling experiments need to be performed using MOF 808 since higher yields were achieved with MOF 808. It has already been reported that higher yield of 5-HMF could be obtained using solvent mixtures in the glucose conversion to 5-HMF. Thus, more solvent-screening experiments should be performed. Furthermore, there is significant scope to attempt other Lewis acid catalysed reactions using MOF 808 or UiO-66 especially if reactions do not form insoluble by-products. If a recyclable catalyst system is developed, it will be possible to conduct reactions under flow conditions to maximize reaction efficiency.